Dear Andrew,

we prepared the revised version of our manuscript. We addressed all reviewer comments as described in detail in our replies below.
At the end of this document we also include the revised paper with tracked changes.

Best regards,

Thomas

Reply to Referee #1

First of all we want to thank this reviewer for the positive assessment and constructive comments. We addressed these comments as explained in detail below.

This manuscript addresses an inconsistency persistently reported in several past studies (some of them by the same authors) between observations of the O4 absorption in atmospheric spectra and radiative transport simulations attempting to reproduce these observations. This inconsistency represents a major issue for the interpretation of MAX-DOAS measurements of aerosol properties, which are based on O4 slant column measurements. Results from past studies indicated that, to reconcile observations with simulations, it is often (but not always) necessary to apply a scaling factor of typically -20% to observations. The reason why this correction is needed remains unknown, but some authors suggested that it might be related to uncertainties in the knowledge of aerosol properties in the atmosphere, which can possibly affect the light path of the solar radiation in a complex way. In the present study, the authors try to overcome this difficulty by concentrating their analysis on observations performed under very low AOD conditions, therefore minimizing uncertainties due to aerosols. Even in such particular conditions, they find that simulations underestimate measurements by about 20%, which confirms that a fundamental inconsistency - not related to aerosols – exists between observations and simulations. Although the study is limited in coverage (only one day of measurements is presented), the proposed case is fully pertinent as it suggests that at least for the conditions of the study inconsistencies cannot be resolved by uncertainties in aerosol properties. The mystery remains however unresolved, since no valid explanation can be proposed. The suggestion that systematic errors on the O4 spectroscopy could be an explanation is on the one hand in contradiction with known uncertainties on laboratory measurements, and on the other hand also in contradiction with published results indicating that a scaling factor is not always required to bring measurements and simulations in good agreement. It would of course be interesting to multiply measurements in similarly low AOD conditions but this is clearly beyond the scope of the paper. From an editorial point of view, the manuscript is concise, well written and well organized. I therefore recommend its publication in AMT, after attention to the few comments listed below.

Many thanks for this positive assessment.

Specific comments

Pg. 5, l. 3: please justify the use of 0.05 as appropriate value for the albedo of the sea at UV wavelengths. A reference would be enough here. Also indicate at which wavelength the radiative transfer calculations have been computed.

We chose the value of 5% to be consistent with the MAPA inversions, and because it is appropriate for many parts of the global ocean. However, by having a closer look at maps of albedo (Kleipool et al., 2008) and chlorophyll content (e.g. from the NASA Earth Observatory:

https://earthobservatory.nasa.gov/global-maps/MY1DMM_CHLORA), we found that at the specific location of the measurements, very clear waters exist, for which the surface albedo is typically higher (about 7 to 8%). The presence of very clear waters is also supported by the in situ chlorophyll measurements made aboard the ship.
We therefore made additional radiative transfer simulations using a surface albedo of 8%. We found that the obtained O_4 dAMFs were almost identical with those obtained for 5% surface albedo (differences <1%). The reason for the good agreement is that the effect of the surface albedo is similar for the O_4 AMFs for different elevation angles. Thus the effect of varying surface albedo almost cancels out.
We added this information to section 6.

Pg. 5, l. 205: I have the impression that the use of lidar backscatter ratio profiles as a proxy for aerosol extinction profiles involves more assumptions than stated here. E.g., one also has to assume that the aerosol phase function does not vary much with altitude, and maybe more important that the backscatter profile shape measured at 1000 nm is also valid at 360nm. But despite all uncertainties, I agree that using ceilometer profiles makes sense in the absence of real extinction values. Maybe the system could be improved by adding a device to measure aerosol surface extinctions (if possible).

Unfortunately, no measurements of aerosol surface extinction are available.
With respect to the representativeness of the measurements at 1064 nm for the MAX-DOAS measurements, we agree with the reviewer that the aerosol properties can change with altitude, and thus the relative profile shape of aerosol extinction at 360 nm might differ from that at 1064 nm.
In order to estimate the effect of the varying aerosol profiles at both wavelengths, we performed additional radiative transfer simulations using modified tropospheric aerosol profiles. The aerosol extinction in the lowest 1000 m of the extracted profiles was changed by +/-20% and the free tropospheric part above was adjusted to keep the total AOD unchanged. The resulting O_4 dAMFs were almost unchanged for elevation angles >4°. For lower elevation angles, the changes were found to be +/-2%.
We added this information to section 6.1.

Pg. 5, l. 221: add a reference to justify the Angström exponent of 2 used for the conversion of the stratospheric AOD (unless this would be documented in Thomason et al., 2018)

We took the value of 2 from existing publications (e.g. Malinina et al., 2019). However, most provided values are representative for larger wavelengths (typically 525 nm or larger). To estimate the uncertainties of the simulated O_4 dSCDs related to the uncertainty of the Angström exponent, we performed additional radiative transfer simulations assuming a stratospheric AOD of 0.008 (corresponding to an Angström exponent of 1). We found that the O_4 dSCDs differ from those for a stratospheric AOD of 0.012 by less than 1%. We added this information to section 6.1.

Pg. 7, sect. 7.2: considering the very low aerosol content, and the comparatively large uncertainty of the assumed stratospheric AOD (basically a climatological value at 525
nm converted to 360 nm using a not well established Angstrom exponent), I think that
the AOD values retrieved by MAPA are highly uncertain. The fact that the retrieved scaling factor matches the values empirically derived in the previous section is not really surprising, since this scaling is already necessary to bring clear-sky simulations in agreement with observations. Inspecting more closely Fig. A13, it seems that the retrieved AOD values are very unstable. Comparing e.g. results derived using SF=0.8 and SF=0.85, we see that AOD values differ quite substantially although RMS values are similar. I am not really convinced that MAPA inversions add a lot of information in the study. At least they are not inconsistent. Something that would be very interesting would be to test whether the discrepancy depends on the O4 wavelength used for the retrieval. Unfortunately, this is not possible using the current setup due to the limited spectral range of the spectrometer, but it should be considered for future studies. Finally, one may also wonder whether this particular day was really the

only clean day (during the ship cruise) allowing for a comparison of measured and simulated O4 slant columns. If other similarly clean days were encountered, it would be nice to know whether similar inconsistencies were found.

We fully agree with the reviewer that the aerosol results from MAPA have large uncertainties.

In the original manuscript, we already wrote: ‚However, here it should be noted that for these low aerosol extinctions, the information content of the measurements is probably too low to constrain the aerosol extinction profiles, especially for high altitudes.'

In the revised version we modified this sentence to: ‚However, here it should be noted that for these low aerosol extinctions, the information content of the measurements is probably too low to constrain the aerosol extinction profiles, especially for high altitudes. Thus also the retrieved AOD values are very unstable (see Fig. A15). Nevertheless, rather clear results for the scaling factor are found:'

For the other two points, we made the following changes:

-other wavelengths:

We added the following sentence at the end of the conclusions: ‚We recommend that similar studies under extremely low aerosol load should be made at different locations and seasons. Also O_4 absorptions at different wavelengths should be investigated.'

-other measurement days:

The extremely low AODs only occurred on the selected day. Only at the beginning of the following day, still low AODs were measured (< 0.05 at 360 nm). However, during this period, the measurements at low elevation angles were strongly affected by clouds. Nevertheless, we compared the MAX-DOAS O_4 measurements retrieved during that period with radiative transfer simulations. Here, we only made simulations for an aerosol-free atmosphere to limit the effort (and also because of the rapid temporal variation of the AOD). The comparison results are shown below:

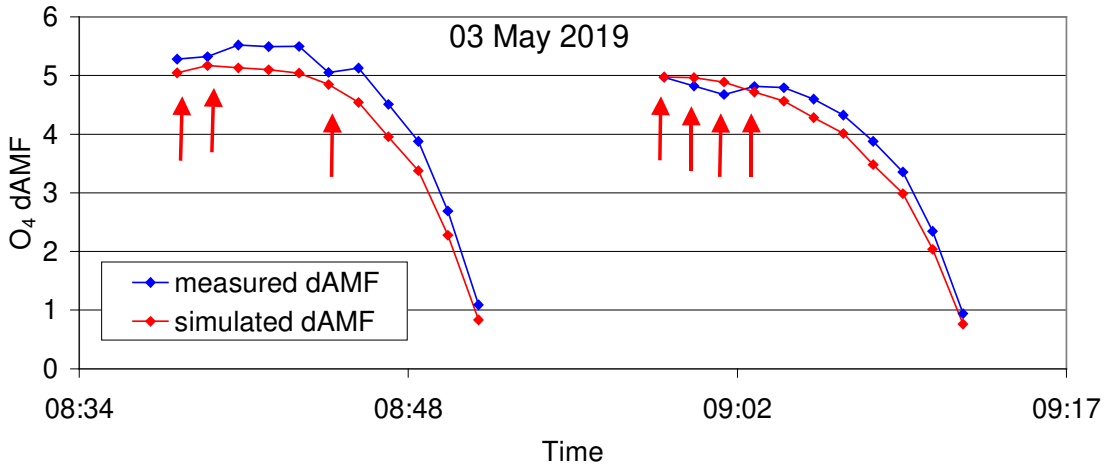

Fig. A13 Comparison of the measured and simulated O_4 dAMFs for two elevation sequences on 05 March 2019. For the first elevation sequence, the AOD was <0.05 at 360 nm. During the second elevation sequence it already increased to 0.06. Note that the radiative transfer simulations were made for an aerosol-free atmosphere.

Like on 02 May 2019, the simulated O_4 dAMFs (for aerosol-free atmosphere) are smaller than the measurements (for cloud-free observations).

We added the following information to section 7.1.:

,It should be noted that during the entire ship cruise, only during the beginning of 3 May 2019, similarly low (but still larger) AOD were measured as on 2 May 2019. We compared the measured O_4 dAMFs for the first two elevation sequences on 3 May with radiative transfer simulations. For that comparison we only made simulations for an aerosol-free atmosphere in order to to limit the effort (and also because of the rapid temporal variation of the AOD during that time period). The results (see Fig. A13) are similar to those on 2 May 2019: Except for the cloud contaminated measurements, the simulations are smaller than the measurements.'

Spelling, typos:

Pg. 1, l. 21: remove 'variation'
Corrected

Pg. 1, l. 33: remove 'mainly'
Corrected

Pg. 3, l. 101: add 'at' between 'are not' and 'the identical location'
Corrected

Pg. 4, l. 151: add 'dry air' between 'For the' and 'mixing ratio of O2'
Corrected

References

Kleipool, Q., Dobber, M., de Haan, J., and Levelt, P., Earth surface reflectance climatology from 3 years of OMI data, J. Geophys. Res.-Atmos., 113, D18308, https://doi.org/10.1029/2008JD010290, 2008.

Malinina, E., Rozanov, A., Rieger, L., Bourassa, A., Bovensmann, H., Burrows, J. P., and Degenstein, D.: Stratospheric aerosol characteristics from space-borne observations: extinction coefficient and Ångström exponent, Atmos. Meas. Tech., 12, 3485–3502, https://doi.org/10.5194/amt-12-3485-2019, 2019.

Reply to Referee #2

First of all we want to thank this reviewer for the positive assessment and constructive comments. We addressed these comments as explained in detail below.

General comments

In recent years, more and more authors have indicated the need for scaling factors in order to improve the agreement of measured and simulated O4 dSCD/dAMF. In the previous publication by Wagner et al. 2019, various factors were investigated to determine the possible cause of this disagreement. One of the key remarks made by reviewers and the community was that the uncertainty of aerosol information and ist impact on the oxygen dimer could not be ruled out as a possible cause of disagreement. In this novel study, Wagner et al. examine the difference of measured and simulated O4 dAMF for low aerosol loads measured during a ship cruise in the Atlantic in 2019. The authors claim that due to the low aerosol load possible aerosol uncertainties can be neglected and that the underlying differences must have another, as yet unknown reason.

The document is well written and structured and the analyses have been carried out thoroughly and consistently. However, I recommend publishing it after making some minor changes listed below.

We thank the reviewer for the positive assessment.

1. Please add a table including all uncertainties described in the document (e.g. pressure/temperature changes, aerosol parameterization, effective temperature, ...)

Many thanks for this good suggestion! We added such a table (new table 3) to the paper:

Table 3 Uncertainties related to the different analysis steps

Spectral analysis		
Effect	**Magnitude**	**Reference**
Spectral fit	1 - 4%	Result of spectral fit
Temperature dependence	1.5%	Wagner et al., 2019
Fit paramaters	3.5%	Appendix A1, and Wagner et al., 2019
Total	4 – 5.5%	
RTM without aerosols		
O_4 profile	1%	Wagner et al., 2019
albedo	1%	Section 6
RTM general	1%	Wagner et al., 2019
total	2%	
RTM with aerosols		
O_4 profile	1%	Wagner et al., 2019
AP & SSA	3%	Section 6
Strat aerosols	1%	Section 6.1
albedo	1%	Section 6
Profile shape	2% for elevation angles < 4°, negligible for higher elevation angles	Section 6.1
RTM general	1%	Wagner et al., 2019
total	4%	
O_4 VCD	2%	This study, section 5, see also Wagner et al., 2019

2. It would be interesting to have a time series of O4 dSCD/dAMF RMS values (similar to A13) for the data shown in Fig.6 and A11. I would expect a clear trend in the RMS differences over the day maybe similar to the one you showed for AOD and scaling factor? How is the correlation of these RMS values and the retrieved/measured AOD?

We prepared the requested figure:

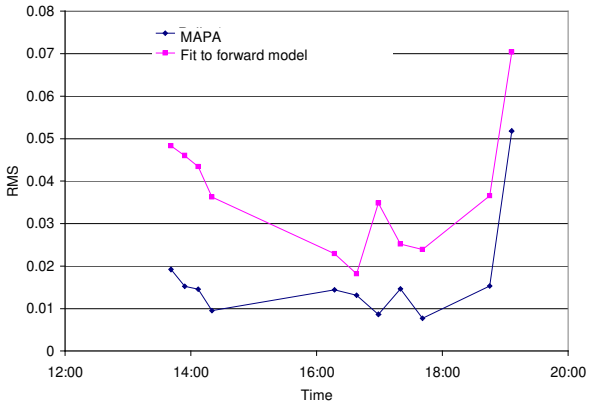

The RMS values from the fit to the forward model show the same temporal trend as the RMS from MAPA, but the absolute values are smaller (as expected).

We also checked the correlation: No correlation was found (R^2=0.00)

3. You mentioned that sun photometer measurements allow to differ between the aerosol particle size. Please show the contribution of differently sized aerosol particles to the total AOD over the day as well as all AODs and corresponding Angström exponents.

The following figure was added (new Fig. A3):

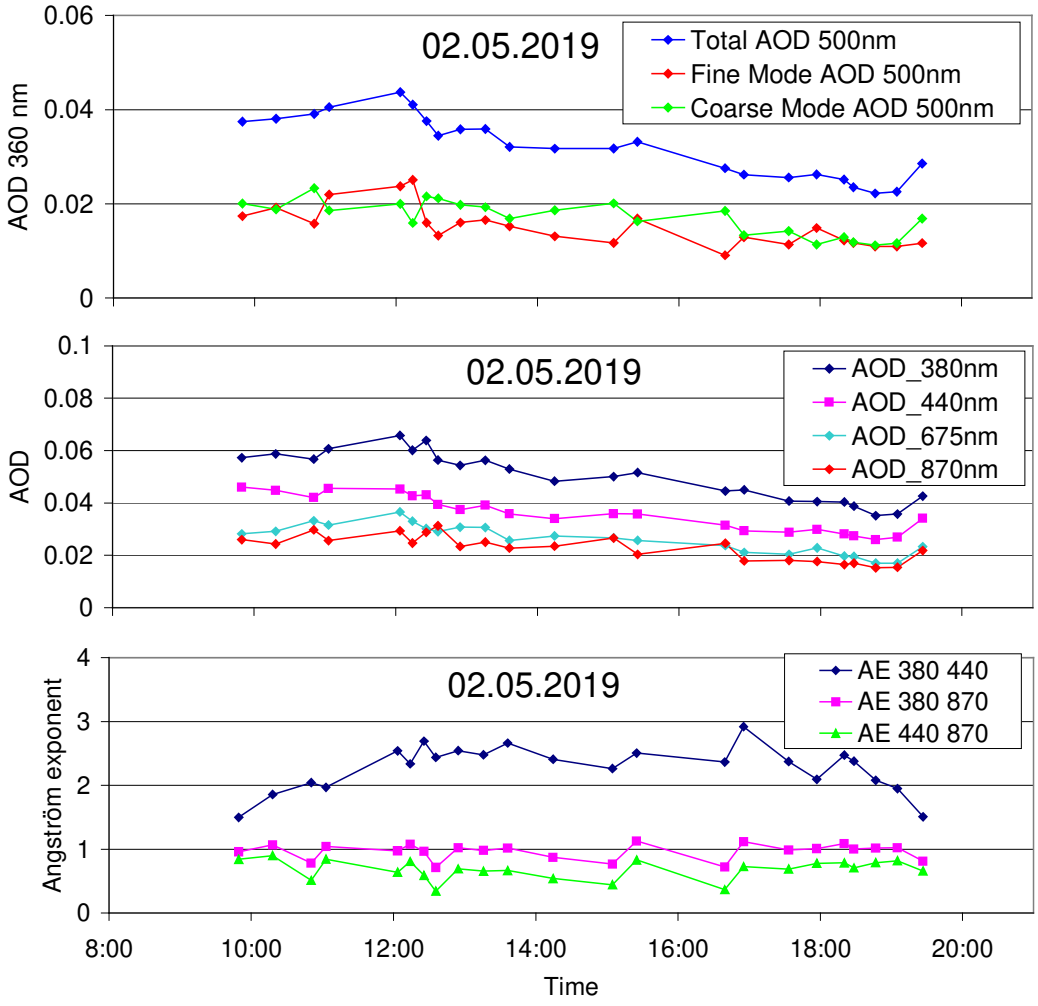

Fig. A3: Top: AOD at 500 nm attributed to the coarse and fine modes, as well as total AOD. Middle: Total AOD at different wavelengths. Bottom: Angström Exponents for selected wavelength pairs.

It should be noted that while creating these figures, it turned out that the AOD for the last measurement on 2 May 2019 (at 19:26) of this fully processed data set was about 30% higher than the value obtained from the initial AOD inversion (while all other measurements on that day were nearly identical). Even after consultation with the AERONET staff, no clear reason for this discrepancy could be identified. However, since the solar zenith angle is rather large (~84°), the extraction of the AOD, especially at short wavelengths is challenging, because of the strong Rayleigh extinction. These uncertainties affect the comparison of the last elevation sequence (19:06 to 19:25).

We added the following information to the paper:

Section 2.2:

‚It should be noted that the uncertainties of the last AOD measurement on 2 May 2019, 19:26, are rather large because of the high SZA of 85°. In particular it was found that for that measurement the AOD from the fully processed sun photometer data (Fig. A3) was about 30% larger than the AOD of the initial retrieval (Fig. 3), while the results for all other measurements are almost identical. The radiative transfer simulations presented below for the last elevation sequence (19:06 to 19:25) are based on the initial (low) AOD values, which are in agreement with AOD measurements 20 minutes earlier. Nevertheless, the comparison results for this last elevation sequence should be treated with caution because of the large uncertainties of the corresponding AOD measurement.'

Figure caption of Fig. 7:

‚Note that for the last elevation sequence, the AOD used in the forward model has large uncertainties, see section 2.2.'

Figure caption of Fig. A12:

‚Note that for the last elevation sequence, the AOD used in the forward model has large uncertainties, see section 2.2.'

4. Furthermore, I was wondering why you only showed results for one day? The AODs for the following days are also rather small. Do these days support your findings?

The extremely low AODs only occurred on the selected day. Only at the beginning of the following day, still low AODs were measured (< 0.05 at 360 nm). However, during this period, the measurements at low elevation angles were strongly affected by clouds. Nevertheless, we compared the MAX-DOAS O_4 measurements retrieved during that period with radiative transfer simulations. Here, we only made simulations for an aerosol-free atmosphere to limit the effort (and also because of the rapid temporal variation of the AOD). The comparison results are shown below:

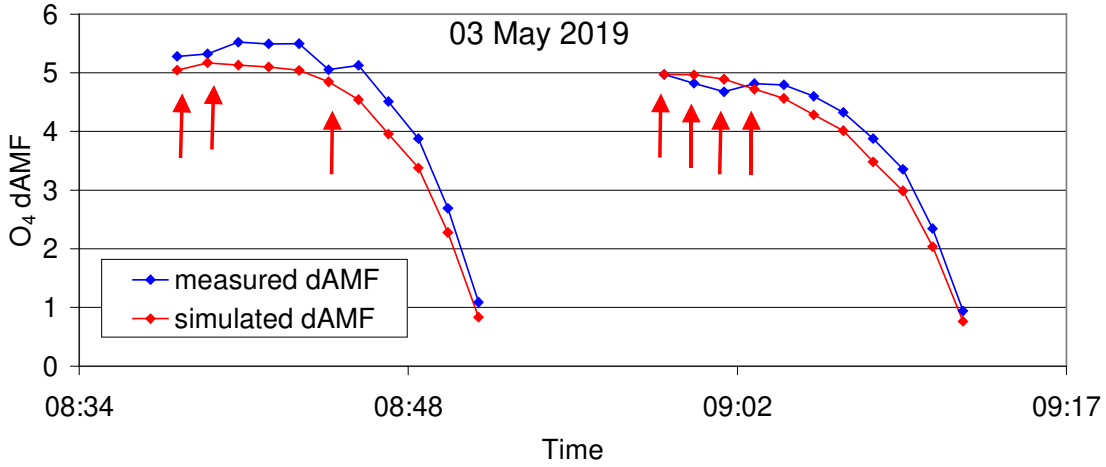

Fig. A13 Comparison of the measured and simulated O_4 dAMFs for two elevation sequences on 05 March 2019, when the AOD was rather small (<0.05 at 360 nm). The radiative transfer simulations were made for an aerosol-free atmosphere.

Like on 02 May 2019, the simulated O_4 dAMFs (for aerosol-free atmosphere) are smaller than the measurements (for cloud-free observations).

We added the following information to section 7.1.:
‚It should be noted that that during the entire ship cruise, only during the beginning of 3 May 2019, similarly low (but still larger) AOD were measured as on 2 May 2019. We also compared the measured O4 dAMFs for the first two elevation sequences on 3 May to radiative transfer simulations. For that comparison we only made simulations for an aerosol-free atmosphere in order to limit the effort (and also because of the rapid temporal variation of the AOD during that time period). The results (see Fig. A13) are similar to those on 2 May 2019: except for the cloud contaminated measurements, the simulations are smaller than the measurements.'

Specific comments

P1, L22, 25: Please add a selection of corresponding references to the sentences starting with (L22) "In recent years,..." and (L25) "Several studies found that a scaling factor...".

We changed the text to:
‚Several studies found that a scaling factor (SF<1) had to be applied to the observed atmospheric O_4 absorptions in order to bring them into agreement with radiative transfer simulations (e.g. Wagner et al., 2009; Clémer et al. 2010). Other studies, however, did not find the need to apply such a scaling factor (e.g. Spinei et al., 2015; Ortega et al., 2016). A more detailed discussion and overview on existing studies of both groups is provided in Wagner et al., 2019.'

We added the following references:

Spinei, E., Cede, A., Herman, J., Mount, G. H., Eloranta, E., Morley, B., Baidar, S., Dix, B., Ortega, I., Koenig, T., and Volkamer, R.: Ground-based direct-sun DOAS and airborne MAX-DOAS measurements of the collision-induced oxygen complex, O2O2, absorption with significant pressure and temperature differences, Atmos. Meas. Tech., 8, 793-809, https://doi.org/10.5194/amt-8-793-2015, 2015.

Wagner, T., Apituley, A., Beirle, S., Dörner, S., Friess, U., Remmers, J., and Shaiganfar, R.: Cloud detection and classification based on MAX-DOAS observations, Atmos. Meas. Tech., 7, 1289-1320, doi:10.5194/amt-7-1289-2014, 2014.

P2, Sec 2.2 and Fig.3: Since AODs at other wavelengths are available, please add them to Fig. 3.

We added a new figure (new Fig. A3) showing the AODs at all wavelengths, see reply to comment 3 above.

P3, L87: "(with..." => "(which...?
Corrected

Fig. A1: Your fit uses the wavelength range 352 - 387nm but Fig. A1 shows only wavelengths up to ~384nm. Please change the x-Axis according to the applied fitting window.

Many thanks for this hint!
In this study, we restricted the spectral range to 352 - 385 nm, because for some measurements (not on 2 May 2019) large spectral structures were found > 385 nm). However, for 2 May 2019, almost identical results (differences < 1%) were found for both spectral ranges.

We added this information to section 3.

The figure below shows the fit results for the spectral range 352 – 387 nm for the same spectrum as shown in Fig. A1. The results are almost identical to those shown in Fig. A1.

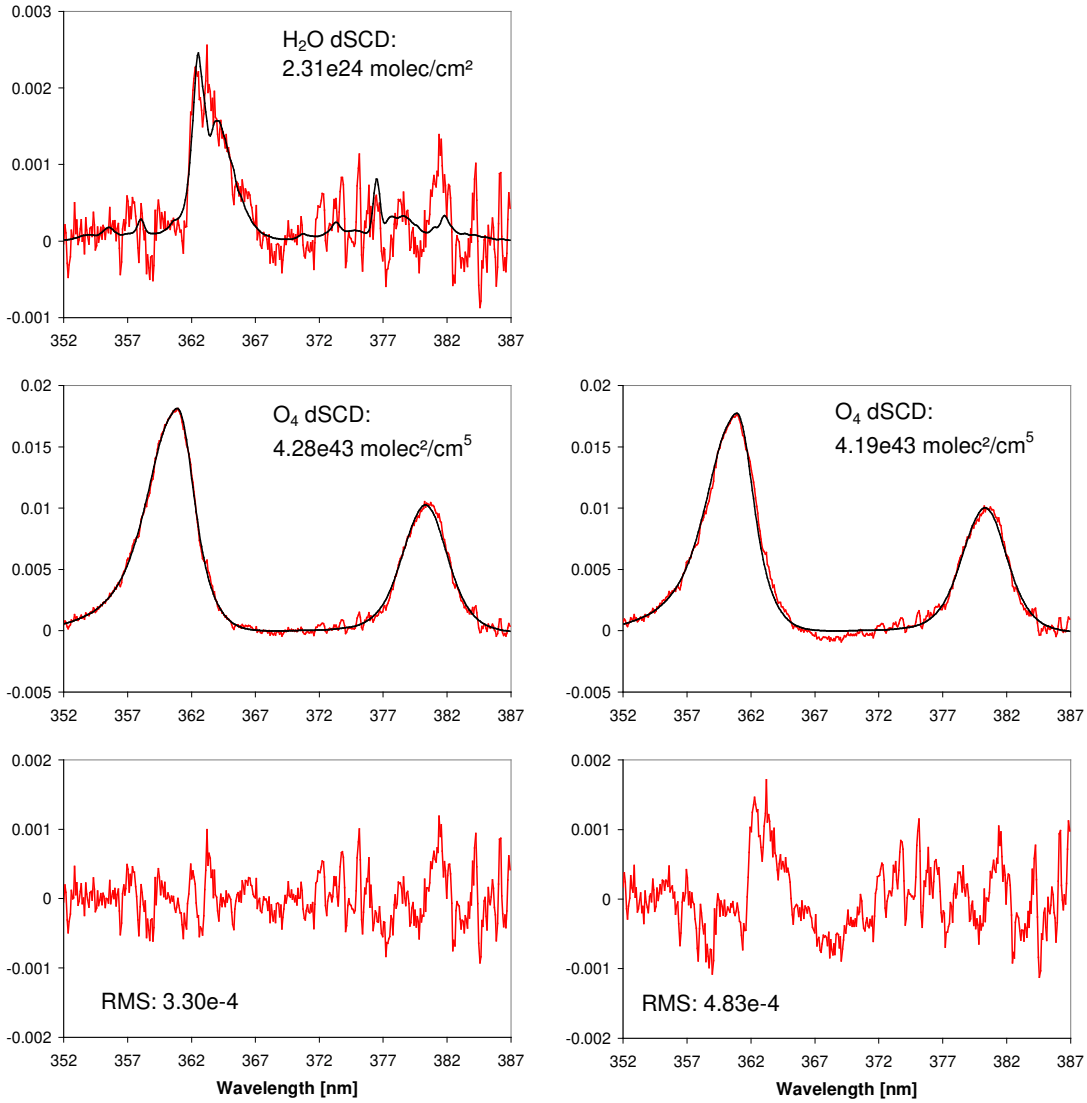

Fit results for a spectrum taken on 2 May 2019, 13:14:50, at an elevation angle of 1° (SZA: 33.6°). Left: results if a H_2O cross section is included in the spectral analysis; right: results if no H_2O cross section is included in the spectral analysis. The black lines represent the fitted cross section, the red lines indicate the residual (bottom) or the residual plus the fitted cross section.

Furthermore, I was wondering about the shown residual. It appears to me that there are still some residual structures left. Especially three peaks around 372-376 nm look familiar and could be attributed to Fraunhofer-Lines. Could this be somehow related to your Ring-treatment or do you have another explanation?

We have no plausible explanation for these structures. For the O4 analysis, these small remaining structures are not critical.

P5, L177: Why was the albedo set to 0.05? Please add a references here. As far as I know, we can expect a small dependence on SZA. How large is the impact on O4 when changing the albedo according to possible values?

We chose the value of 5% to be consistent with the MAPA inversions, and because it is appropriate for many parts of the global ocean. However, by having a closer look at maps of albedo (Kleipool et al., 2008) and chlorophyll content (e.g. from the NASA Earth Observatory: https://earthobservatory.nasa.gov/global-maps/MY1DMM_CHLORA), we found that at the specific

location of the measurements, very clear waters exist, for which the surface albedo is typically higher (about 7 to 8%). The presence of very clear waters is also supported by the in situ chlorophyll measurements made aboard the ship.

We therefore made additional radiative transfer simulations using a surface albedo of 8%. We found that the obtained O_4 dAMFs were almost identical with those obtained for 5% surface albedo (differences <1%). The reason for the good agreement is that the effect of the surface albedo is similar for the O_4 AMFs for different elevation angles. Thus the effect of varying surface albedo almost cancels out.

We added this information to section 6.

P6, L215: "the the", please remove either first or second "the".

We removed both the first and second ‚the' and added a new one.

P6, L216: You wrote that Fig. A8 includes constant and linearly extrapolated values for lower altitudes but the greenish line does not look like a linear extrapolation to me.
Why is that?

Many thanks for this hint. We corrected the figure.

P6, L221: Why is the Angström exponent "assumed" to be 2 when you have AODs at several wavelengths available to calculate more accurate values?

The AOD measurements represent the total AOD, but what is needed is the Angström exponent for the stratospheric aerosols. Therefore, the sun photometer measurements cannot be used for that purpose.

P6, L224: decsribed => described
Corrected

P7, L263: "smaller than" => "larger than"
Corrected

P7, L276: "bebetween" => "be between"
Corrected

Fig. A7 Could you please add a similar figure for the geometry with the smallest RAA to better assess the impact of AP and SSA variations throughout the day?

The figure for 13:30 (RAA ~0) is added.

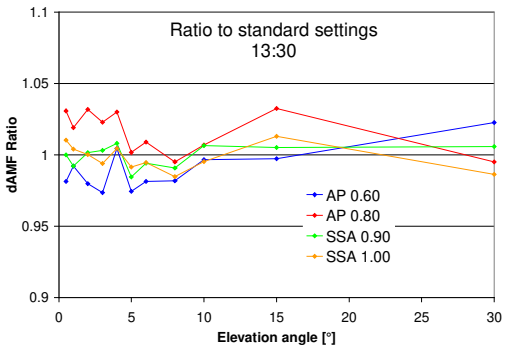

Reply to Referee #3

First of all we want to thank this reviewer for the positive assessment and constructive comments. We addressed these comments as explained in detail below.

The present manuscript addresses the issue of the difference between measured and simulated O4 dSCDS. Many studies over the last year used correction factors on the measured O4 dSCDs to achieve a better agreement without finding the physical explanation of these factors. Other studies support that the use of correction factor is not necessary. In previous studies, one possible explanation of this inconsistency was the uncertainties of aerosol information. It is very interesting that in this manuscript, this uncertainty is neglected because of the use of one day of measurements with very low AOD values. I recommend the publication of the present manuscript. The content is clear, well explained and the manuscript falls into the scope of AMT.

Many thanks for the positive assessment.

Please consider some minor comments:

1. In Figure 1, I see that other days (or at least time windows during some days) have very small AOD values. Why these days are not included in your results? Would it be possible to include them and see if the results agree with the main findings of your study?

The extremely low AODs only occurred on the selected day. Only at the beginning of the following day, still low AODs were measured (< 0.05 at 360 nm). However, during this period, the measurements at low elevation angles were strongly affected by clouds. Nevertheless, we compared the MAX-DOAS O_4 measurements retrieved during that period with radiative transfer simulations. Here, we only made simulations for an aerosol-free atmosphere to limit the effort (and also because of the rapid temporal variation of the AOD). The comparison results are shown below:

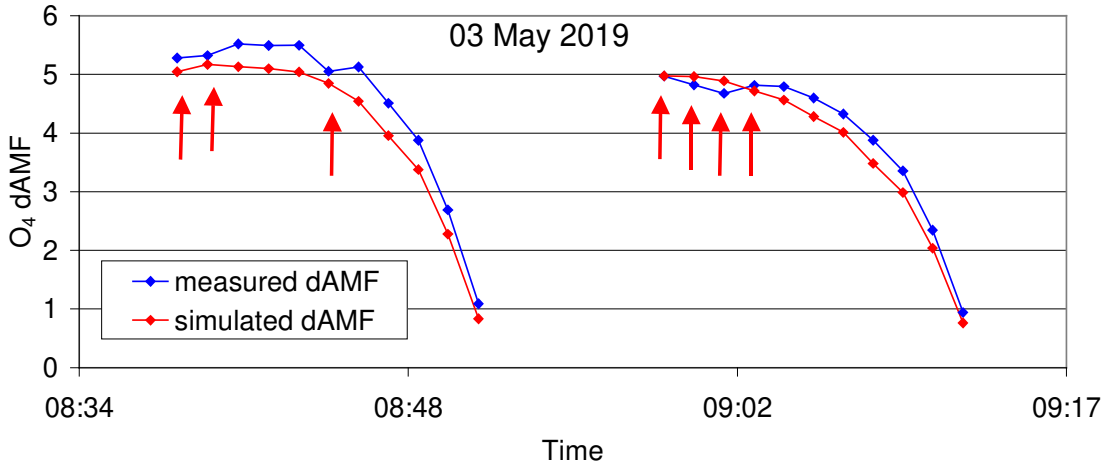

Fig. A13 Comparison of the measured and simulated O_4 dAMFs for two elevation sequences on 05 March 2019, when the AOD was rather small (<0.05 at 360 nm). The radiative transfer simulations were made for an aerosol-free atmosphere.

Like on 02 May 2019, the simulated O_4 dAMFs (for aerosol-free atmosphere) are smaller than the measurements (for cloud-free observations).

We added the following information to section 7.1.:
‚It should be noted that that during the entire ship cruise, only during the beginning of 3 May 2019, similarly low (but still larger) AOD were measured as on 2 May 2019. We also compared the measured

O4 dAMFs for the first two elevation sequences on 3 May to radiative transfer simulations. For that comparison we only made simulations for an aerosol-free atmosphere in order to limit the effort (and also because of the rapid temporal variation of the AOD during that time period). The results (see Fig. A13) are similar to those on 2 May 2019: except for the cloud contaminated measurements, the simulations are smaller than the measurements.'

2. The uncertainties that are described in the text are very important for your findings. That would be very useful if you could create a table of uncertainties.

A new table (table 3) was added to the paper (at the end of section 7.2):

Table 3 Uncertainties related to the different analysis steps

Spectral analysis		
Effect	**Magnitude**	**Reference**
Spectral fit	1 - 4%	Result of spectral fit
Temperature dependence	1.5%	Wagner et al., 2019
Fit paramaters	3.5%	Appendix A1, and Wagner et al., 2019
Total	4 – 5.5%	
RTM without aerosols		
O_4 profile	1%	Wagner et al., 2019
albedo	1%	Section 6
RTM general	1%	Wagner et al., 2019
total	2%	
RTM with aerosols		
O_4 profile	1%	Wagner et al., 2019
AP & SSA	3%	Section 6
Strat aerosols	1%	Section 6.1
albedo	1%	Section 6
Profile shape	2% for elevation angles < 4°, negligible for higher elevation angles	Section 6.1
RTM general	1%	Wagner et al., 2019
total	4%	
O_4 VCD	2%	This study, section 5, see also Wagner et al., 2019

Specific comments:
1. P.1, Line 21 : "aside from" instead of "aside"
Corrected

2. P.1, Line 22 : "e.g.," instead of "e.g."
Corrected

3. P. 1, Line 32 : "In this study," instead of "In this study"
Corrected

4. P. 1, Line 25 : Please add some studies that used a scaling factor

We changed the text to:
‚Several studies found that a scaling factor (SF<1) had to be applied to the observed atmospheric O4 absorptions in order to bring them into agreement with radiative transfer simulations (e.g. Wagner et al., 2009; Clémer et al. 2010). Other studies, however, did not find the need to apply such a scaling factor (e.g. Spinei et al., 2015; Ortega et al., 2016). A more detailed discussion and overview on existing studies of both groups is provided in Wagner et al., 2019.'

We added the following references:

Spinei, E., Cede, A., Herman, J., Mount, G. H., Eloranta, E., Morley, B., Baidar, S., Dix, B., Ortega, I., Koenig, T., and Volkamer, R.: Ground-based direct-sun DOAS and airborne MAX-DOAS measurements of the collision-induced oxygen complex, O2O2, absorption with significant pressure and temperature differences, Atmos. Meas. Tech., 8, 793-809, https://doi.org/10.5194/amt-8-793-2015, 2015.

Wagner, T., Apituley, A., Beirle, S., Dörner, S., Friess, U., Remmers, J., and Shaiganfar, R.: Cloud detection and classification based on MAX-DOAS observations, Atmos. Meas. Tech., 7, 1289-1320, doi:10.5194/amt-7-1289-2014, 2014.

5. P. 4, Line 156 : Can you provide a possible explanation for this difference between ECMWF and in-situ measurements?

The most probable reasons for the discrepancies are originating from the rather coarse horizontal (~80 km) and temporal (6 h) resolution of the ECMWF interim data set: First, the given model data is the average for the modelled box. Moreover, the simulation uncertainties are increased for parameterized subscale processes (e.g. wave motion) which do affect the in-situ measurements.
This information is added to section 5.

6. P. 5, Line 175 : "simulations," instead of "simulations"
Corrected

7. P. 5, Line 208, 210, Figure 4 : Is there any explanation why the raw data vary more with altitude? Is it valid to use the data above 3 km?

We added the following information to the figure caption:

‚The scatter of the range corrected backscatter profiles increases, because the received raw signal scales with the inverse of the square of the distance.'

We used the profile data for altitudes, for which the signal stays positive (after smoothing). The exact altitude, at which the signal is set to zero has negligible influence on the simulated O_4 dAMFs.

We added this information to section 6.1.

8. Figure A8 : y axis varies from 0 km to 10 km and not from 0 km to 0 km. Please correct
Corrected

9. P. 6, Line 221 : why the Angstrom coefficient is assumed equal to 2?

We took the value of 2 from existing publications (e.g. Malinina et al., 2019). However, most provided values are representative for larger wavelengths (typically 525 nm or larger). To estimate the uncertainties of the simulated O_4 dSCDs related to the uncertainty of the Angström exponent, we performed additional radiative transfer simulations assuming a stratospheric AOD of 0.008 (corresponding to an Angström exponent of 1). We found that the O_4 dSCDs differ from those for a stratospheric AOD of 0.012 by less than 1%. We added this information to the paper.

10. P. 7, Line 276 : “be between” instead of “bebetween”
Corrected

Quantitative comparison of measured and simulated O_4 absorptions for one day with extremely low aerosol load over the tropical Atlantic

Thomas Wagner[1], Steffen Dörner[1], Steffen Beirle[1], Sebastian Donner[1], Stefan Kinne[2]
[1]Satellite Remote Sensing Group, Max Planck Institute for Chemistry, Mainz, Germany
[2]Max-Planck Institute for Meteorology, Hamburg, Germany

Correspondence to: Thomas Wagner (thomas.wagner@mpic.de)

Abstract. In this study we compare measured and simulated O_4 absorptions for conditions of extremely low aerosol optical depth (between 0.034 to 0.056 at 360nm) on one day during a ship cruise in the tropical Atlantic. For such conditions, the uncertainties related to imperfect knowledge of aerosol properties don't significantly affect the comparison results. We find that the simulations underestimate the measurements by 15% to 20%. Even for simulations without any aerosols the measured O_4 absorptions are still systematically higher than the simulation results. The observed discrepancies can not be explained by uncertainties of the measurements and simulations and thus indicate a fundamental inconsistency between simulations and measurements.

1 Introduction

Remote sensing measurements of the atmospheric absorption of the oxygen dimer $(O_2)_2$ are often used to derive properties of aerosols and clouds. The atmospheric concentration of $(O_2)_2$ (in the following referred to as O_4) varies only slightly with temperature, pressure and humidity ~~variations~~ (aside from the dependence on altitude). Thus deviations from the O_4 absorptions for clear sky conditions indicate changes of the atmospheric radiative transfer, e.g., due to clouds and aerosols. In recent years, inconsistencies between the measured atmospheric O_4 absorption and radiative transfer simulations were detected for Multi-AXis-DOAS (MAX-DOAS) observations. MAX-DOAS instruments measure scattered sun light under different, mostly slant elevation angles (Hönninger and Platt, 2002). Several studies found that a scaling factor (SF<1) had to be applied to the observed atmospheric O_4 absorptions in order to bring them into agreement with radiative transfer simulations (e.g. Wagner et al., 2009; Clémer et al. 2010). Other studies, however, did not find the need to apply such a scaling factor (e.g. Spinei et al., 2015; Ortega et al., 2016). A more detailed discussion and overview on existing studies of both groups is provided ~~; see also discussion~~ in Wagner et al., 2019~~, and references therein~~). One major difficulty in the quantitative interpretation of these comparisons is that usually the atmospheric aerosol properties are not well known (e.g. the vertical extinction profile and/or the optical properties). And even if they were known, it is still a challenge to accurately represent them in atmospheric radiative transfer simulations.

In this study, we ~~mainly~~ minimise these difficulties by using atmospheric observations in the presence of very low aerosol loads. During a ship campaign across the tropical Atlantic, very low aerosol optical depth (AOD) was observed on one day (2 May 2019). At 360 nm (the wavelength at which we analyse the atmospheric O_4 absorption), the AOD ranged from 0.034 to 0.056, which is an order of magnitude lower than the optical depth of molecular Rayleigh scattering.

Like in previous studies, we compare the observed atmospheric O_4 absorption with the results of radiative transfer simulations. Information about the aerosol properties is derived from sun photometer measurements in combination with ceilometer measurements. Also in our study, considerable uncertainties about the aerosol vertical profile and the aerosol optical properties exist. However, these uncertainties are less important for the interpretation of the comparison results than in previous studies because of the low AOD, and we find large discrepancies between the measured and simulated O_4 absorptions.

The paper is organised as follows: In section 2, an overview on the ship campaign and the instruments used in this study is given. Sections 3 to 5 describe the spectral analysis, the cloud classification, and the calculation of the O_4 profile. In section

6, the radiative transfer simulations and the extraction of the aerosol extinction profiles are presented. Section 7 presents the comparison results, and section 8 the summary and conclusions.

2 Overview on the ship campaign and the instruments used in this study

The MAX-DOAS measurements were carried out during a cruise (MSM82/2) of the German research vessel RV Maria S. Merian (https://www.ldf.uni-hamburg.de/merian.html) from Montevideo (Uruguay) to Las Palmas (Spain) from 26 April 2019 to 14 May 2019 (see Fig. 1). More details on the ship cruise MSM82/2 can be found in Krastel et al. (2019). In this study, we focus on one day with particularly low AOD (2nd May), which is marked in Fig. 1.

The MAX-DOAS instrument was mounted above the ship's bridge at about 20m altitude above sea level. The telescope was aligned in the driving direction of the ship (Fig. 2).

2.1 MAX-DOAS instrument

The MAX-DOAS instrument is a so-called Tube MAX-DOAS instrument which was developed and built by the electronic workshop of the Max Planck Institute for Chemistry in Mainz (Donner, 2016). It consists of two major parts: the telescope unit and the spectrometer unit. The telescope unit is mounted outside on the railing of the ship. The spectrometer unit is located inside the ship. Besides the spectrometer it also contains a peltier cooling element which stabilises the spectrometer temperature at 15 °C. Both units are connected via a quartz glass fibre bundle and electric cables. The telescope unit is equipped with a gyroscope to stabilise the elevation angles by continuously adjusting the motor position with an accuracy of ±0.1°.

The spectrometer is an Avantes ULS2048x64-USB2. It covers the spectral range from 299.4 nm to 463.1 nm with a spectral resolution between 0.52 and 0.54 nm as described by the full width half maximum (FWHM). Spectra are measured with an integration time of 1 min at the following elevation angles: -2°, -1°, -0.5°, 0°, 0.5°, 1°, 2°, 3°, 4°, 5°, 6°, 8°, 10°, 15°, 30°, 90°. Note that in this study only measurements with positive elevation angles are used. One elevation sequence is completed within about 21 min. Dark current and offset spectra are taken during night and are used to correct the measured spectra before the spectral analysis.

2.2 Sun photometer

A MICROTOPS II sunphotometer provided atmospheric totals on aerosol and water vapor. The instrument, when directed towards the sun (in a handheld operation), captures via diodes the solar intensity in five sub-spectral bands near wavelengths of 380, 440, ~~670~~675, 870 and 940 nm. In combination with the larger reference solar intensity at the top of the atmosphere - using time and (GPS-provided) position data - sun-photometer measurements define the atmospheric attenuation at these solar sub-spectral bands. Four spectral bands (near 380, 440, ~~670~~ 675 and 870 nm) sample in trace-gas poor regions, while one spectral band (near 940nm) is strongly affected by water vapor absorption. In the absence of clouds, the solar attenuations in the four trace-gas poor bands can be linked to aerosol - after (surface air pressure defined) contributions from air-molecule (Rayleigh) scattering have been removed. Hereby, the aerosol associated attenuations are quantified by the (vertically normalized) aerosol optical depth (AOD). As the instrument offers AOD values simultaneously at four different solar wavelengths, the typical aerosol particle size is revealed and even AOD contributions from sub-micrometer (mainly from pollution and wildfire) and super-micrometer size aerosol particles (mainly from dust and seasalt) can be distinguished. The determination of the atmospheric water vapor is based on the differential absorption between 870 and 940 nm attenuation data. Any quality measurement usually relies on many repeated samples in order to identify and remove poor

data associated with sun-view contamination by clouds and/or inaccurate orientations of the instrument into the sun (~~with~~ which is done manually with the help of a pointing device). NASA's Aeronet sub-group of the Maritime Aerosol Network (MAN, Smirnov et al., 2009) provided the calibrated instrument for the cruise and also stores cruise data at https://aeronet.gsfc.nasa.gov/new_web/cruises_new/Maria_Merian_19_0.html.

The AOD at 360 nm for 2 May 2019 is shown in Fig. 3. Other results from the sun photometer measurements (AODs at different wavelengths, Angström exponents, and fine and coarse mode AOD) are presented in Fig. A3).

It should be noted that the uncertainties of the last AOD measurement on 2 May 2019, 19:26, are rather large because of the high SZA of 85°. In particular it was found that for that measurement the AOD from the fully processed sun photometer data (Fig. A3) was about 30% larger than the AOD of the initial retrieval (Fig. 3), while the results for all other measurements are almost identical. The radiative transfer simulations presented below for the last elevation sequence (19:06 to 19:25) are based on the initial (low) AOD values, which are in agreement with AOD measurements 20 minutes earlier. Nevertheless, the comparison results for this last elevation sequence should be treated with caution because of the large uncertainties of the corresponding AOD measurement.

2.3 Ceilometer

The Jenoptik 15K ceilometer of the MPI-M is a simple laser system operating at 1064nm, at an invisible trace-gas free near-IR wavelength. Laser impulses are sent upward into the atmosphere and based on strength and delay of backscattered return signals altitude positions for atmospheric aerosol and clouds are derived. Due to their stronger backscatter at optically thicker media, such as clouds, overhead cloud base altitudes are well captured. However, as laser light strongly attenuates in optically thicker media, no information above a cloud base is possible. Vertical profiles of aerosol for clouds-free views (and below clouds) are possible up to about 7km in altitude during the night but only up to about 4km in altitude during the day, due to scattering noise by sunlight. No useful aerosol profiling is possible near the surface (e.g. lower 300m), because signal sender and receiver are not at the identical location. Recorded ceilometer data of the cruise are accessible via an anonymous ftp-site at ftp://ftp-projects.zmaw.de/aerocom/ships/ceilometer_MSM/.

3 Spectral analysis

The spectral analysis is performed following mostly the settings suggested by Wagner et al. (2019). The spectral range from 352 to ~~387~~ 385 nm is chosen, which contains two O_4 absorption bands. Note that in Wagner et al. (2019) the wavelength range 352 – 387 nm was used. Here we restricted it to 352 - 385 nm, because for some measurements (not on 2 May 2019) large spectral structures were found > 385 nm). For 2 May 2019, almost identical results (differences < 1%) were found for both spectral ranges. The details of the analysis are given in Table 1. Fig. A1 (left) presents an example of the spectral analysis as used in this study. In addition to the other cross sections, also a H_2O cross section (Polyansky et al. 2018) is included. The reason for including a H_2O cross section as well as the effect of including a second O_4 cross section are discussed in appendix A1.

The results of the spectral analysis represent the integrated trace gas concentration along the atmospheric light path, the so-called slant column density (SCD). For O_4 the SCD is expressed with respect to the square of the O_2 concentration (see Greenblatt et al., 1990). Thus, the unit of the O_4 SCD is molec²/cm^5. For the analysis of the measured spectra, a so-called Fraunhofer reference spectrum is used. In this study, the Fraunhofer reference spectrum is calculated as the average of the zenith spectra before and after the chosen elevation sequence, weighted by the time of the selected measurement from that elevation sequence. Before performing the spectral analysis, these sequential Fraunhofer reference spectra are fitted to a ‚universal' Fraunhofer reference spectrum (29 April 13:43, SZA: 44.8°, elevation angle: 90°) to transfer the spectral

calibration of the universal Fraunhofer reference spectrum to the sequential Fraunhofer reference spectra. The universal Fraunhofer reference spectrum was calibrated using a high resolved solar spectrum.

Since the Fraunhofer reference spectrum also contains atmospheric trace gas absorptions, the output of the spectral analysis represents the difference between the SCDs of the selected non-zenith spectrum and the Fraunhofer reference spectrum, the so-called differential SCD (or dSCD).

The typical fit error of the derived O_4 dSCD is between $2 \cdot 10^{41}$ molec^2/cm^5 and $4 \cdot 10^{41}$ molec^2/cm^5. Depending on the magnitude of the retrieved O_4 dSCD this corresponds to relative errors between 1 and 4 %.

4 Cloud detection using the MAX-DOAS measurements

Although during most of the afternoon on 2 May clear sky conditions prevailed, also some scattered clouds were present. They were e.g. detected by the ceilometer in zenith direction (see Fig. 3). In order to derive information about possible cloud contamination for the individual MAX-DOAS measurements, the MAX-DOAS measurements themselves were used for the detection of cloud contamination, similar as in Wagner et al., (2014, 2016). Figure ~~A3~~ A4 in the appendix shows the time series of the retrieved O_4 dSCDs on 2 May for the different elevation angles. During the morning the O_4 dSCDs show strong variability caused by the presence and variability of clouds as also seen in the ceilometer data (Fig. 3). During the afternoon, for most of the time, smooth variations of the O_4 dSCDs are found indicating clear sky conditions. However, for some times and elevation angles, also small systematic deviations (usually reductions) of the O_4 dSCDs occur, which are caused by scattered clouds. During periods without any cloud contamination, the temporal variability of the retrieved O_4 dSCDs is rather small (scatter of the O_4 dSCDs is typically $\leq 5 \cdot 10^{41}$ molec^2/cm^5). Measurements with deviations $> 10^{42}$ molec^2/cm^5 compared to the extrapolated O_4 SCDs from the smooth (cloud-free) neighboring measurements are thus flagged as cloud-contaminated. From the selected 11 elevation sequences during the mainly cloud-free periods in the afternoon of 2 May, 7 are found to be completely free of cloud contamination.

5 Calculation of the O_4 profile and O_4 VCD

The O_4 height profile and VCD for 2 May 2019 are calculated from vertical profiles of temperature and pressure. Also the effect of the atmospheric humidity is accounted for. For the profiles of temperature, pressure and atmospheric humidity we used the results from the ECMWF ERA-Interim data set (Berrisford et al., 2011) for 2 May 2019. From the temperature and pressure profiles the air concentration [air] is calculated. Then the O_2 concentration $[O_2]$ is derived according to the following equation:

$$[O_2] = [air] \cdot M_{O2} \cdot (1 - M_{H2O}) \quad (1)$$

Here M_{H2O} is the mixing ratio of water vapour taken from the ERA interim data. For the dry air mixing ratio of O_2 (M_{O2}) a value of 21% is assumed. The O_4 concentration is then represented by the square of the O_2 concentration (Greenblatt et al., 1990). To derive the O_4 VCD, the O_4 concentration is vertically integrated between the surface and 30 km with a vertical resolution of 20 m.

The temperature and pressure from the ECMWF ERA-Interim data set at the surface are also compared to the in situ measurements on the ship. It is found that the ECMWF temperature is slightly lower (-0.7 K) and the ECMWF pressure is slightly higher (+2 hPa) than the corresponding in situ measurements, see Fig. ~~A4~~ A5 in the appendix. Therefore, we repeated our calculations of the O_4 profiles by shifting the ECMWF values for the whole profiles by +0.7 K and – 2 hPa. The resulting change of the O_4 VCD is rather small (+0.3 %). The derived O_4 VCD for the modified profile is (1.245 ± 0.25)

$\cdot 10^{43}$molec^2/cm^5. The most probable reasons for the discrepancies are originating from the rather coarse horizontal (~80 km) and temporal (6 h) resolution of the ECMWF interim data set: First, the given model data is the average for the modelled box. Moreover, the simulation uncertainties are increased for parameterized subscale processes (e.g. wave motion) which do affect the in-situ measurements.

To estimate the uncertainty of the derived O_4 VCD the temperature and pressure of the whole profiles are varied by ±2 K and ±2 hPa, respectively. The resulting changes of the O_4 VCDs are ±1.5 % and ±0.9 %, respectively. In addition, assuming an uncertainty of the atmospheric humidity profile of 30% leads to an uncertainty of the derived O_4 VCD of 0.9 %. Thus, we estimate the total uncertainty of the O_4 VCD to ±2 %.

Finally, a subtle detail should be mentioned: the integration of the O_4 VCD was performed starting from sea level, while the instrument was located about 20 m above sea level. This rather small difference would result in a reduction of the O_4 VCD by 0.4 %. However, this effect is considered in exactly the same way in the radiative transfer simulations, where the instrument was also put at an altitude of 20 m, while the O_4 AMFs are calculated for the O_4 column starting from sea level. Thus it is a consistent procedure to use the O_4 VCD integrated from sea level for the conversion of the measured O_4 dSCDs into O_4 dAMFs.

6 Radiative transfer simulations

O_4 dSCDs are calculated using the full spherical Monte Carlo radiative transfer model MCARTIM (Deutschmann et al. 2011). For the simulations, the profiles of temperature, pressure, and O_4 as described in section 5 are used. The vertical resolution was set to 20 m close to the surface and increases with altitude (see Table 2). The surface albedo was set to 0.05. The value of 5% was chosen to be consistent with the MAPA inversions, and because it is appropriate for many parts of the global ocean. However, by having a closer look at maps of albedo (Kleipool et al., 2008) and chlorophyll content (e.g. from the NASA Earth Observatory: https://earthobservatory.nasa.gov/global-maps/MY1DMM_CHLORA), we found that at the specific location of the measurements, very clear waters exist, for which the surface albedo is typically higher (about 7 to 8 %). The presence of very clear waters was also supported by the in situ chlorophyll measurements aboard the ship. We therefore made additional radiative transfer simulations using a surface albedo of 8 %. We found that the obtained O_4 dAMFs were almost identical with those for 5 % surface albedo (differences <1%). The reason for the good agreement is that the effect of the surface albedo is similar for the O_4 AMFs for different elevation angles. Thus the effect of varying surface albedo almost cancels out.

The simulations were performed for the exact SZA and relative azimuth angles of the individual measurements. From the obtained O_4 AMFs, the corresponding O_4 dAMFs are calculated by subtracting the simulated O_4 AMFs for the zenith viewing direction. To achieve best consistency with the measurements, for the simulation of the zenith measurements (interpolated between the zenith observations before and after the sequence) the SZA and relative azimuth angle for the exact time of the non-zenith measurements are also used for the simulations of the zenith measurements. The temporal evolution of the SZA and relative azimuth angle for 2 May are shown in Fig. ~~A5~~ A6 in the appendix.

It should be noted that it is important to use a consistent treatment of the SZA and relative azimuth angles in the simulations and measurement analyses. Especially the choice of the Fraunhofer reference spectra is important. If e.g. either zenith measurements before or after the selected elevation sequence are used as reference spectra, systematic deviations of the retrieved O_4 dSCDs of up to 10% can occur (see Fig. ~~A6~~ A7 in the appendix).

O_4 dAMFs are simulated for two aerosol extinction profiles as well as for a pure Rayleigh atmosphere. For the extraction of the aerosol extinction profiles, the observations by the sun photometer and the ceilometer were used (see section 6.1). For the simulations including aerosols, the phase function is represented by a Henyey-Greenstein (HG) parameterisation with an asymmetry parameter of 0.68. The single scattering albedo was set to 0.95. Variations of these properties lead to changes of

the simulated O_4 dSCDs by up to ±3 % (see Fig. ~~A7~~ A8 in the appendix). These rather low uncertainties are related to the low AOD on 2 May 2019. For measurements with higher aerosol loads, the corresponding uncertainties are usually much larger (e.g. Wagner et al., 2019). Here it should be noted that the HG phase function model is a rather simplified approximation for true aerosol phase functions. Thus especially for measurements with small scattering angles (e.g. around noon on 2 May 2019) the uncertainties of the RTM simulations might be larger.

6.1 Extraction of the aerosol extinction profiles

Figure 4 presents the hourly averaged and range corrected ceilometer backscatter profiles for three periods in the afternoon on 2 May 2019 without cloud contamination. In a first order approximation, these backscatter profiles are proportional to the aerosol extinction. Thus together with the total AOD from the sun photometer measurements, the aerosol extinction profiles can be determined. However, ceilometer measurements are affected by several instrumental limitations, which complicate the direct conversion to aerosol extinction profiles:

a) Due to the missing overlap between the outgoing beam and the field of view of the detector, the sensitivity of the ceilometer is very low for altitudes below 500 m. Thus for this altitude range, no information on the aerosol extinction can be derived from the ceilometer measurements.

b) In spite of the long averaging period, still strong noise appears for altitudes above 3 km.

Due to these limitations, the ceilometer profiles can only be used for a restricted altitude range. In the following we used the ceilometer profiles for the altitude range between 500 m and about 7 to 9 km. Between 500 m and 3000 m, averages for 100 m layers are calculated. Below 500 m, the values at 500 m are either set constant for the layer below, or are linearly extrapolated from the ceilometer data between 500 m and 800 m (similar as in Wagner et al., 2019). Since between 3 km and 10 km the noise increases strongly, a third order polynomial was fitted to the ceilometer data in that height range. The polynomial values are used for the altitude range for which positive values are obtained. Between 7 and 9 km the polynomial values for the three profiles cross zero. Above these altitudes, ~~the the~~ the profile values are set to zero. These extraction steps are illustrated in Fig. ~~A8~~ A9 in the appendix. Here it should be noted that the exact choice of the altitude, at which the extinction is set to zero, has negligible influence of the simulated O_4 dAMFs.

Before the backscatter profiles are normalised with the total AODs measured by the sun photometer, the stratospheric part of the total aerosol profile has to be added. This step is usually not important, because in more polluted areas the total AOD is clearly dominated by the tropospheric part. However, for our study, the total AOD is so low that the stratospheric part constitutes a substantial fraction (up to 25 %) of the total AOD. Thomason et al. (2018) report the stratospheric AODs in the Tropics at 525 nm to be about 0.005 to 0.006. Assuming an Angström exponent of 2 (e.g. Malinina et al., 2019) the corresponding AOD at 360 nm is estimated to around 0.011 and 0.013. In the following we used a value of 0.012. Here it should be noted that the Angström exponent for stratospheric aerosols is usually derived for wavelengths at and above 525 nm. Thus it is not clear how representative the used value of 2 is also for shorter wavelengths. To estimate the uncertainties of the simulated O_4 dSCDs related to the uncertainty of the Angström exponent, we performed additional radiative transfer simulations assuming a stratospheric AOD of 0.008 (corresponding to an Angström exponent of about 1). We found that the O_4 dSCDs differ from those for a stratspheric AOD of 0.012 by less than 1%.

This ~~value~~ stratospheric AOD (0.012) is then subtracted from the total AOD (Fig. 3) measured by the sun photometer. Then the tropospheric aerosol profiles (as described above, see also Fig. ~~A8~~A9) are normalised by the resulting tropospheric AOD. Finally, the stratospheric extinction profile is added to the normalised tropospheric aerosol extinction profiles. For the stratospheric extinction profile we used a simplified shape with an AOD of 0.012. Here it is important to note that the details of the extinction profile in the upper troposphere and stratosphere are not critical. For example, the simulated O_4 dAMFs

using aerosol profiles with or without the stratospheric part are almost the same. The final aerosol extinction profiles used for the RTM simulations are shown in Fig. 4.

It should be noted that the aerosol properties can change with altitude. Thus the relative profile shape measured at 1064 nm might differ from the aerosol extinction profile at 360 nm. In order to estimate the effect of the varying aerosol profiles at both wavelengths, we performed additional radiative transfer simulations using modified tropospheric aerosol profiles. The aerosol extinction in the lowest 1000 m of the extracted profiles was changed by +/-20% and the free tropospheric part above was adjusted to keep the total AOD unchanged. The resulting O_4 dAMFs were almost unchanged for elevation agles >4°. For lower elevation angles, the changes were found to be +/-2%.

6.2 Calculation of effective temperatures for the O_4 absorption

Since the temperature of the troposphere decreases with altitude, and the O_4 absorption cross section depends on temperature, the retrieved O_4 dSCDs might deviate from the true O_4 dSCDs (the integrated O_4 concentration along the atmospheric light paths), because only one O_4 cross section for a fixed temperature is used in the spectral analysis. Thus, before the O_4 dAMFs from the measured spectra are compared to those from the radiative transfer simulations, the effect of the temperature dependence of the O_4 absorption has to be investigated.

The effective temperature of the O_4 measurements is calculated according to:

$$T_{eff,\alpha} = \frac{\sum_z [O_4]_z \cdot (bAMF_{z,\alpha} - bAMF_{z,90°}) \cdot T_z}{\sum_z [O_4]_z \cdot (bAMF_{z,\alpha} - bAMF_{z,90°})} \quad (2)$$

Here $[O_4]_z$ represents the O_4 concentration at altitude z, $bAMF_{z,\alpha}$ the box-AMF for elevation angle α at altitude z, and T_z the temperature at altitude z. $T_{eff,\alpha}$ is the effective temperature for the measured O_4 dSCD at elevation angle α.

Equation 2 is applied for each individual measurement, the results are shown in Fig. ~~A9~~A10. The effective temperatures range from 276 K to 299 K. They depend systematically on the elevation angle and SZA. Measurements at low elevation angles are most sensitive for the layers near the surface, at which the highest temperatures occur. Measurements at high SZA (towards the end of the considered time period) have higher sensitivities for higher atmospheric layers with colder temperatures. Both dependencies are well represented by the results shown in Fig. ~~A9~~A10.

To correct the effect of the temperature dependence, the correction factors presented in Fig. 13 in Wagner et al. (2019) are applied to the O_4 dSCDs retrieved with the O_4 cross section for 293 K. The corrected O_4 dSCDs differ by up to a few percent (between –2 % and +7 %) from the original O_4 dSCDs. In Fig. ~~A10~~ A11 in the appendix the effect of the temperature correction is shown for two selected elevation sequences. For the comparison with the radiative transfer simulations the temperature-corrected O_4 dSCDs (or dAMFs) are used.

7 Comparison results

7.1 Direct comparison between measurements and RTM results

In Fig. 6 the O_4 dAMFs derived from the MAX-DOAS measurements are compared to those obtained from the radiative transfer simulations for elevation sequences not affected by clouds (similar comparisons for the sequences with cloud-contaminated measurements are shown in Fig. ~~A11~~ A12 in the appendix).

In the left part of Fig. 6, the results from radiative transfer simulations without aerosols are shown. Here, for almost all cases, the measured O_4 dAMFs are systematically ~~smaller~~ larger than the simulated O_4 dAMFs. This is an important finding, because especially for the low elevation angles, the presence of aerosol scattering leads to a decrease of the O_4 dSCDs. Thus the simulations for a pure Rayleigh atmosphere represent an upper limit of the achievable O_4 dSCDs. Only for cloudy cases with a high probability for multiple scattering events higher O_4 dSCDs could occur, but such conditions can be ruled out here because of the absence of thick and vertically extended clouds. Thus the overestimation of the simulated O_4 dSCDs for a pure Rayleigh atmosphere by the measured O_4 dSCDs indicates a fundamental inconsistency between measurements and simulations. Similar results are found for the elevation sequences with cloud contamination (Fig. ~~A11~~ A12 in the appendix).

In the right part of Fig. 6, simulation results for the aerosol profiles extracted in section 6.1 are shown. Note the separate y-axes for the simulated O_4 dAMFs on the right side, for which the maxima are chosen to achieve best agreement between the measured and simulated O_4 dAMFs. The exact values of the axis maxima were determined by fitting the measured O_4 dAMFs to the simulated O_4 dAMFs for elevation angles >4°. For these elevation angles the simulation results for the different profile shapes below 500m) are almost the same. Good qualitative agreement between measurements and simulation is found, especially for the aerosol profiles with constant extinction below 500 m. However, the absolute values differ strongly. The ratios between measured and simulated O_4 dAMFs are found to b~~eb~~etween 0.8 and 0.86. Again, similar results are found for the elevation sequences with cloud contamination (Fig. ~~A11~~ A12 in the appendix).

The scaling factors derived from this comparison between measured and simulated O_4 dSCDs are presented as blue data points in Fig. 7.

It should be noted that during the entire ship cruise, only during the beginning of 3 May 2019, similarly low (but still larger) AOD were measured as on 2 May 2019. We compared the measured O_4 dAMFs for the first two elevation sequences on 3 May with radiative transfer simulations. For that comparison we only made simulations for an aerosol-free atmosphere in order to limit the effort (and also because of the rapid temporal variation of the AOD during that time period). The results (see Fig. A13) are similar to those on 2 May 2019: Except for the cloud contaminated measurements, the simulations are smaller than the measurements.

7.2 Profile inversion with MAPA

We also applied our profile inversion algorithm, the Mainz profile algorithm (MAPA, Beirle et al., 2019), to the measured O_4 dAMFs. For that purpose, a new MAPA LUT had to be created, because the lowest AOD in the original LUT (0.05) is larger than all AODs observed on 2 May 2020. The new LUT includes AOD values from zero to 0.1 in steps of 0.02. MAPA provides the option to apply a fixed user-defined scaling factor, or to determine a scaling factor yielding best match between forward model and measurement during profile inversion.

In Fig. ~~A12~~ A14 in the appendix the retrieved extinction profiles are shown for different scaling factors. Here it should be noted that the individual measurements (not the sequences) with cloud contamination were skipped before the profile inversion. Only profiles with either ‚valid' or ‚warning' flags are shown (profiles with ‚error' flags are not shown). In Fig. ~~A13~~ A15 in the appendix the retrieved AODs for the different scaling factors are compared to the tropospheric AODs from the sun photometer measurements (stratospheric AOD of 0.012 was subtracted). Also the RMS between the measured and simulated O_4 dAMFs are shown (right). The colour of the MAX-DOAS inversion results indicates the quality of the profile inversion.

Most valid profiles are obtained for scaling factors between 0.80 and 0.90, or for a free fitted (variable) scaling factor. For the inversions with larger scaling factors, rather high RMS are found. For most cases, the retrieved AODs are smaller than those measured by the sun photometer. However, here it should be noted that for these low aerosol extinctions, the information content of the measurements is probably too low to constrain the aerosol extinction profiles, especially for high

altitudes. Thus also the retrieved AOD values are very unstable (see Fig. A15).~~However, here it should be noted that for these low aerosol extinctions, the information content of the measurements is probably too low to constrain the aerosol extinction profiles, especially for high altitudes~~.

The obtained scaling factors are shown in Fig. 7. Overall good agreement between both comparison methods is found. For all elevation sequences, values of the scaling factor < 1 are found. For the direct comparison, the difference from unity is mostly larger than 15 % and can thus not be explained by the uncertainties of the measurements and simulations, which are summarised in table 3..

8 Conclusions

We compared measured and simulated O_4 absorptions for one day with very low aerosol optical depth. For such conditions, the uncertainties caused by imperfect knowledge of the aerosol properties play a smaller role than for comparison under more polluted conditions.

One important result of the comparison was that for all measurements, the observed O_4 absorption was higher than the simulation results for an atmosphere without aerosols. In the absence of optically thick clouds, the simulated O_4 dAMFs for an atmosphere without aerosols constitutes an upper limit, since especially for the low elevation angles the inclusion of aerosols leads to a decrease of the O_4 absorption. The observed discrepancies thus indicate a fundamental inconsistency between simulations and measurements.

The measured O_4 absorptions are also compared to simulations including aerosol extinction profiles. The aerosol extinction profiles were constrained by measurements of the sun photometer, the ceilometer and a climatology of stratospheric aerosols. Again, a large discrepancy was found for the absolute values. However, for the relative dependence of the O_4 dAMFs on the elevation angle good agreement could be achieved. For each elevation sequence, the ratio of simulated and measured O_4 dAMFs was calculated. For that purpose the elevation angles >4° were used, for which the O_4 dAMFs are almost insensitive to the profile shape in the lower atmospheric layers. For all elevation sequences, ratios of 0.85 or less were found. Similar ratios were also obtained from the application of our profile inversion algorithm (MAPA) to the measurements. The observed discrepancies cannot be explained by the uncertainties of measurements and/or simulations. Here it is important to note that in the spectral analysis, we explicitly corrected for the (small) temperature dependence of the atmospheric O_4 absorption.

Our results indicate that something fundamental is missing/wrong in either the radiative transfer simulations or the spectral analysis of the atmospheric O_4 absorptions. We did not find a clear reason for the discrepancies. One possible reason for the discrepancies could be a systematically too small O_4 absorption cross section.

We recommend that similar studies under extremely low aerosol load should be made at different locations and seasons. Also O_4 absorptions at different wavelengths should be investigated.

Author contributions

T. Wagner performed the measurements, data analysis and prepared the manuscript. S. Dörner prepared the MAX-DOAS instrument and extracted the ERA interim data. S. Dörner and S. Donner contributed to the MAX-DOAS operation and data analysis. S. Beirle performed the MAPA profile inversions. S. Kinne operated the sun photometer and ceilometer.

Acknowledgements

The scientific party of RV MARIA S. MERIAN Cruise MSM82/2 gratefully acknowledges the very friendly and most effective cooperation with Captain Maaß and his crew. Their great flexibility and their perfect technical assistance

substantially contributed to make this cruise a scientific success. We also appreciate the valuable support by the Leitstelle Deutsche Forschungsschiffe (German Research Fleet Coordination Centre) at the University of Hamburg. The expedition was funded by the Deutsche Forschungsgemeinschaft.

References

Bogumil, K., J. Orphal, T. Homann, S. Voigt, P.Spietz, O.C. Fleischmann, A. Vogel, M. Hartmann, H. Bovensmann, J. Frerik and J.P. Burrows, Measurements of Molecular Absorption Spectra with the SCIAMACHY Pre-Flight Model: Instrument Characterization and Reference Data for Atmospheric Remote-Sensing in the 230-2380 nm Region, J. Photochem. Photobiol. A., 157, 167-184, 2003.

Beirle, S., Dörner, S., Donner, S., Remmers, J., Wang, Y., and Wagner, T.: The Mainz profile algorithm (MAPA), Atmos. Meas. Tech., 12, 1785–1806, https://doi.org/10.5194/amt-12-1785-2019, 2019.

Berrisford, P, Dee, DP, Poli, P, Brugge, R, Fielding, M, Fuentes, M, Kållberg, PW, Kobayashi, S, Uppala, S, Simmons, A, The ERA-Interim archive Version 2.0, ERA Report Series No.1 Version 2.0 (https://www.ecmwf.int/node/8174), 2011.

Chen, Z., Bhartia, P. K., Torres, O., Jaross, G., Loughman, R., DeLand, M., Colarco, P., Damadeo, R., and Taha, G.: Evaluation of the OMPS/LP stratospheric aerosol extinction product using SAGE III/ISS observations, Atmos. Meas. Tech., 13, 3471–3485, https://doi.org/10.5194/amt-13-3471-2020, 2020.

Deutschmann, T., Beirle, S., Frieß, U., Grzegorski, M., Kern, C., Kritten, L., Platt, U., Pukite, J., Wagner, T., Werner, B., and Pfeilsticker, K.: The Monte Carlo Atmospheric Radiative Transfer Model McArtim: Introduction and Validation of Jacobians and 3D Features, J. Quant. Spectrosc. Ra., 112, 1119–1137, doi:10.1016/j.jqsrt.2010.12.009, 2011.

Donner, S.: Mobile MAX-DOAS measurements of the tropospheric formaldehyde column in the Rhein-Main region, Master's thesis, University of Mainz, http://hdl.handle.net/11858/00-001M-0000-002C-EB17-2, 2016.

Greenblatt G.D., Orlando, J.J., Burkholder, J.B., and Ravishankara, A.R.: Absorption measurements of oxygen between 330 and 1140 nm, J. Geophys. Res., 95, 18577-18582, 1990.

Hönninger, G. and Platt, U.: Observations of BrO and its vertical distribution during surface ozone depletion at Alert, Atmospheric Environment, 36, 2481 – 2489, 2002.

Kleipool, Q., Dobber, M., de Haan, J., and Levelt, P., Earth surface reflectance climatology from 3 years of OMI data, J. Geophys. Res.-Atmos., 113, D18308, https://doi.org/10.1029/2008JD010290, 2008.

Krastel, S., RV Maria S. Merian-Cruise MSM82/2, short cruise report, German Research Fleet Coordination Centre, University of Hamburg (https://www.ldf.uni-hamburg.de/merian/wochenberichte/wochenberichte-merian/msm82-2-msm84/msm82-2-scr.pdf), 2019.

Lampel, J., Pöhler, D., Polyansky, O. L., Kyuberis, A. A., Zobov, N. F., Tennyson, J., Lodi, L., Frieß, U., Wang, Y., Beirle, S., Platt, U., and Wagner, T.: Detection of water vapour absorption around 363 nm in measured atmospheric absorption spectra and its effect on DOAS evaluations, Atmos. Chem. Phys., 17, 1271-1295, https://doi.org/10.5194/acp-17-1271-2017, 2017.

Malinina, E., Rozanov, A., Rieger, L., Bourassa, A., Bovensmann, H., Burrows, J. P., and Degenstein, D.: Stratospheric aerosol characteristics from space-borne observations: extinction coefficient and Ångström exponent, Atmos. Meas. Tech., 12, 3485–3502, https://doi.org/10.5194/amt-12-3485-2019, 2019.

Ortega, I., Berg, L. K., Ferrare, R. A., Hair, J. W., Hostetler, C. A., and Volkamer, R.: Elevated aerosol layers modify the O2-O2 absorption measured by ground-based MAX-DOAS, J. Quant. Spectrosc. Ra., 176, 34–49, https://doi.org/10.1016/j.jqsrt.2016.02.021, 2016.

Polyansky, O.L., A.A. Kyuberis, N.F. Zobov, J. Tennyson, S.N. Yurchenko and L. Lodi ExoMol molecular line lists XXX: a complete high-accuracy line list for water, Monthly Notices of the Royal Astronomical Society , 480 (2), 2597-2608, 2018.

Spinei, E., Cede, A., Herman, J., Mount, G. H., Eloranta, E., Morley, B., Baidar, S., Dix, B., Ortega, I., Koenig, T., and Volkamer, R.: Ground-based direct-sun DOAS and airborne MAX-DOAS measurements of the collision-induced oxygen complex, O2O2, absorption with significant pressure and temperature differences, Atmos. Meas. Tech., 8, 793-809, https://doi.org/10.5194/amt-8-793-2015, 2015.

Smirnov, A., B. N. Holben, I. Slutsker, D. M. Giles, C. R. McClain, T. F. Eck, S. M. Sakerin, A. Macke, P. Croot, G. Zibordi, P. K. Quinn, J. Sciare, S. Kinne, M. Harvey, T. J. Smyth, S. Piketh, T. Zielinski, A. Proshutinsky, J. I. Goes, N. B. Nelson, P. Larouche, V. F. Radionov, P. Goloub, K. Krishna Moorthy, R. Matarrese, E. J. Robertson, and F. Jourdin Maritime Aerosol Network as a component of Aerosol Robotic Network, J. Geophys. Res., 114, D06204, doi:10.1029/2008JD011257, 2009.

Thalman, R. and Volkamer, R.: Temperature dependent absorption cross-sections of O_2–O_2 collision pairs between 340 and 630 nm and at atmospherically relevant pressure, Phys. Chem. Chem. Phys., 15, 15371, doi:10.1039/c3cp50968k, 2013.

Thomason, L. W., Ernest, N., Millán, L., Rieger, L., Bourassa, A., Vernier, J.-P., Manney, G., Luo, B., Arfeuille, F., and Peter, T.: A global space-based stratospheric aerosol climatology: 1979–2016, Earth Syst. Sci. Data, 10, 469–492, https://doi.org/10.5194/essd-10-469-2018, 2018.

Vandaele, A. C., C. Hermans, P. C. Simon, M. Carleer, R. Colin, S. Fally, M.-F. Mérienne, A. Jenouvrier, and B. Coquart, Measurements of the NO2 Absorption Cross-section from 42000 cm-1 to 10000 cm-1 (238-1000 nm) at 220 K and 294 K, J. Quant. Spectrosc. Radiat. Transfer, 59, 171-184, 1997.

Wagner, T., Deutschmann, T., and Platt, U.: Determination of aerosol properties from MAX-DOAS observations of the Ring effect, Atmos. Meas. Tech., 2, 495-512, 2009.

~~Wagner, T., Beirle, S., and Deutschmann, T.: Three-dimensional simulation of the Ring effect in observations of scattered sun light using Monte Carlo radiative transfer models, Atmos. Meas. Tech., 2, 113-124, 2009.~~

Wagner, T., Apituley, A., Beirle, S., Dörner, S., Friess, U., Remmers, J., and Shaiganfar, R.: Cloud detection and classification based on MAX-DOAS observations, Atmos. Meas. Tech., 7, 1289-1320, doi:10.5194/amt-7-1289-2014, 2014.

Wagner, T., Apituley, A., Beirle, S., Dörner, S., Friess, U., Remmers, J., and Shaiganfar, R.: Cloud detection and classification based on MAX-DOAS observations, Atmos. Meas. Tech., 7, 1289-1320, doi:10.5194/amt-7-1289-2014, 2014.

Wagner, T., Beirle, S., Remmers, J., Shaiganfar, R., and Wang, Y.: Absolute calibration of the colour index and O_4 absorption derived from Multi AXis (MAX-) DOAS measurements and their application to a standardised cloud classification algorithm, Atmos. Meas. Tech., 9, 4803-4823, doi:10.5194/amt-9-4803-2016, 2016.

Wagner, T., Beirle, S., Benavent, N., Bösch, T., Chan, K. L., Donner, S., Dörner, S., Fayt, C., Frieß, U., García-Nieto, D., Gielen, C., González-Bartolome, D., Gomez, L., Hendrick, F., Henzing, B., Jin, J. L., Lampel, J., Ma, J., Mies, K., Navarro, M., Peters, E., Pinardi, G., Puentedura, O., Puķīte, J., Remmers, J., Richter, A., Saiz-Lopez, A., Shaiganfar, R., Sihler, H., Van Roozendael, M., Wang, Y., and Yela, M.: Is a scaling factor required to obtain closure between measured and modelled atmospheric O_4 absorptions? An assessment of uncertainties of measurements and radiative transfer simulations for 2 selected days during the MAD-CAT campaign, Atmos. Meas. Tech., 12, 2745–2817, https://doi.org/10.5194/amt-12-2745-2019, 2019.

Wang, Y., Beirle, S., Hendrick, F., Hilboll, A., Jin, J., Kyuberis, A. A., Lampel, J., Li, A., Luo, Y., Lodi, L., Ma, J., Navarro, M., Ortega, I., Peters, E., Polyansky, O. L., Remmers, J., Richter, A., Puentedura, O., Van Roozendael, M., Seyler, A., Tennyson, J., Volkamer, R., Xie, P., Zobov, N. F., and Wagner, T.: MAX-DOAS measurements of HONO slant column densities during the MAD-CAT campaign: inter-comparison, sensitivity studies on spectral analysis settings, and error budget, Atmos. Meas. Tech., 10, 3719-3742, https://doi.org/10.5194/amt-10-3719-2017, 2017.

Wang, Y., Apituley, A., Bais, A., Beirle, S., Benavent, N., Borovski, A., Bruchkouski, I., Chan, K. L., Donner, S., Drosoglou, T., Finkenzeller, H., Friedrich, M. M., Frieß, U., Garcia-Nieto, D., Gómez-Martín, L., Hendrick, F., Hilboll, A., Jin, J., Johnston, P., Koenig, T. K., Kreher, K., Kumar, V., Kyuberis, A., Lampel, J., Liu, C., Liu, H., Ma, J., Polyansky, O. L., Postylyakov, O., Querel, R., Saiz-Lopez, A., Schmitt, S., Tian, X., Tirpitz, J.-L., Van Roozendael, M., Volkamer, R., Wang, Z., Xie, P., Xing, C., Xu, J., Yela, M., Zhang, C., and Wagner, T.: Inter-comparison of MAX-DOAS measurements of tropospheric HONO slant column densities and vertical profiles during the CINDI-2 campaign, Atmos. Meas. Tech., 13, 5087–5116, https://doi.org/10.5194/amt-13-5087-2020, 2020.

Tables

Table 1: Settings for the DOAS analysis of O_4

Parameter	**Value, Remark / Reference**
Spectral range	352 – 387 nm
Degree of DOAS polynomial	5
Degree of intensity offset polynomial	2
Fraunhofer reference spectrum	Interpolated between 90° measurement before and after each elevation sequence
Wavelength calibration	Fit to high resolution solar spectrum using Gaussian slit function
Shift / squeeze	The measured spectrum is shifted and squeezed against all other spectra
Ring spectrum 1	Normal Ring spectrum calculated from measured zenith spectrum
Ring spectrum 2	Ring spectrum 1 multiplied by λ^{-4} (Wagner et al. (2009)
O_3 cross section	223 K, Bogumil et al. (2003)
NO_2 cross section	294 K, Vandaele et al. (1997)
H_2O cross section	293 K, Polyansky et al. (2018)
O_4 cross section	293 K, Thalman and Volkamer (2013)

Table 2: Vertical resolution used for the radiative transfer simulations

Altitude range [km]	Vertical resolution [km]
0 - 0.5	0.02
0.5 - 2	0.1
2 – 12	0.2
12 – 25	1
25 – 45	2
45 - 100	5

Table 3: Uncertainties related to the different analysis steps

Spectral analysis		
Effect	**Magnitude**	**Reference**
Spectral fit	1 - 4%	Result of spectral fit
Temperature dependence	1.5%	Wagner et al., 2019
Fit paramaters	3.5%	Appendix A1, and Wagner et al., 2019
Total	4 – 5.5%	
RTM without aerosols		
O_4 profile	1%	Wagner et al., 2019
albedo	1%	Section 6
RTM general	1%	Wagner et al., 2019
total	2%	
RTM with aerosols		
O_4 profile	1%	Wagner et al., 2019
AP & SSA	3%	Section 6
Strat aerosols	1%	Section 6.1
albedo	1%	Section 6
Profile shape	2% for elevation angles < 4°, negligible for higher elevation angles	Section 6.1
RTM general	1%	Wagner et al., 2019
total	4%	
O_4 VCD	2%	This study, section 5, see also Wagner et al., 2019

Figures

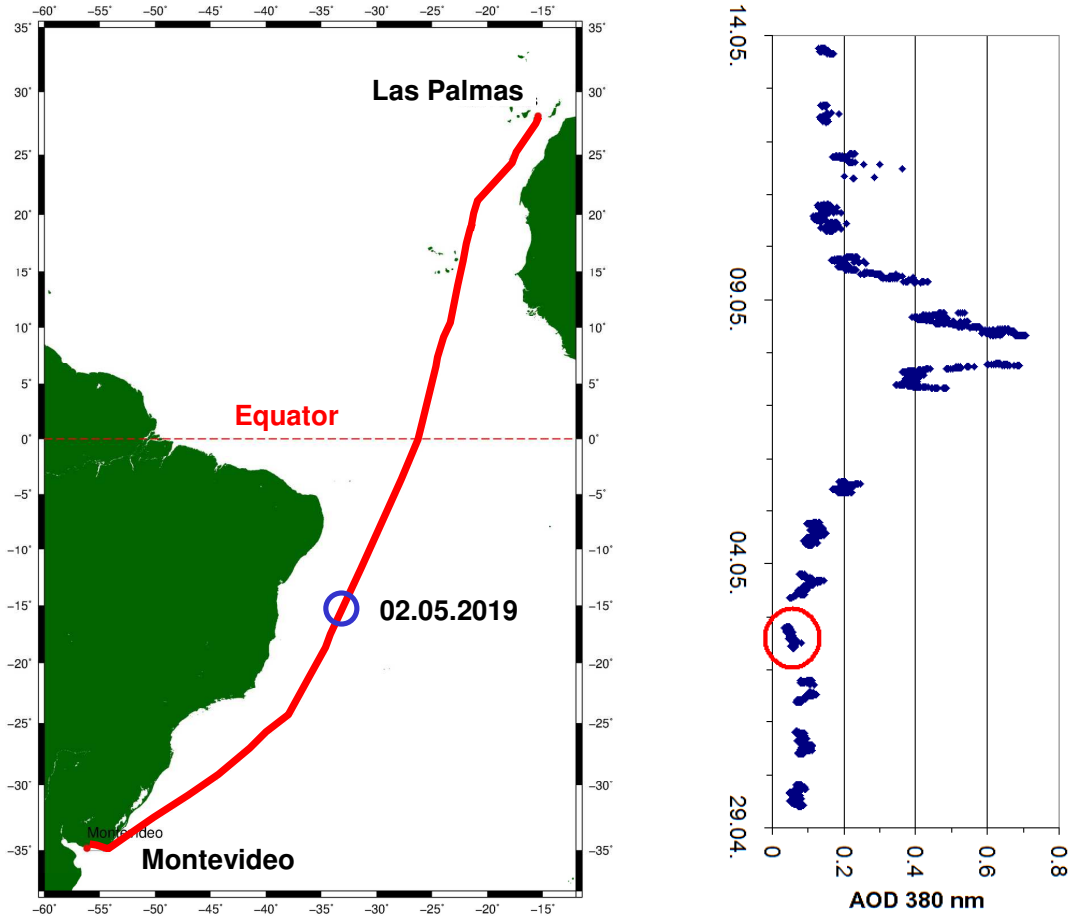

Fig. 1: Left: Ship route from Montevideo to Las Palmas. The blue circle indicates the location of the measurements used in this study. Right: Aerosol optical depth at 380 nm measured with a hand-held sun photometer.

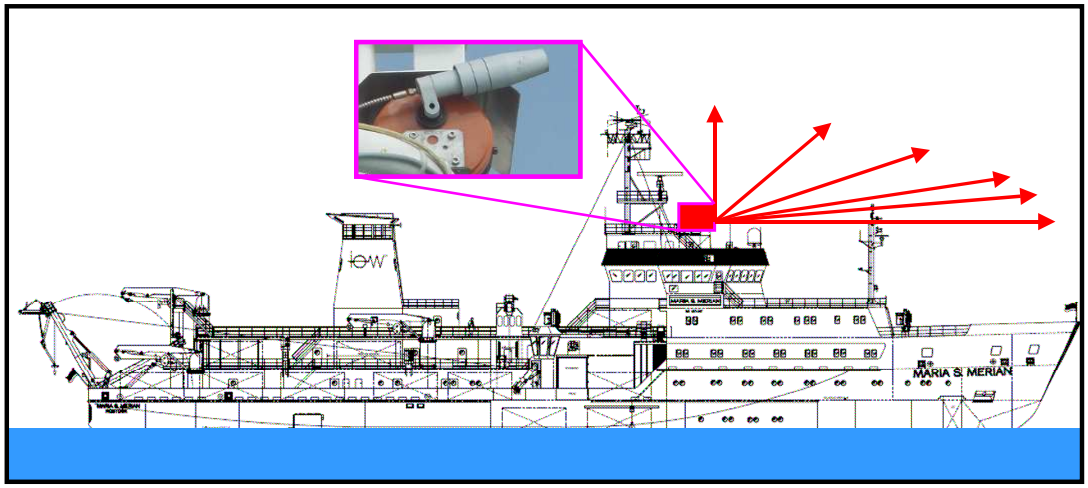

Fig. 2: The position and viewing direction of the MAX-DOAS instrument on the RV Maria S. Merian during the ship cruise (ship drawing taken from https://briese-research.de/research-department/research-vessels/rv-maria-s-merian).

1205

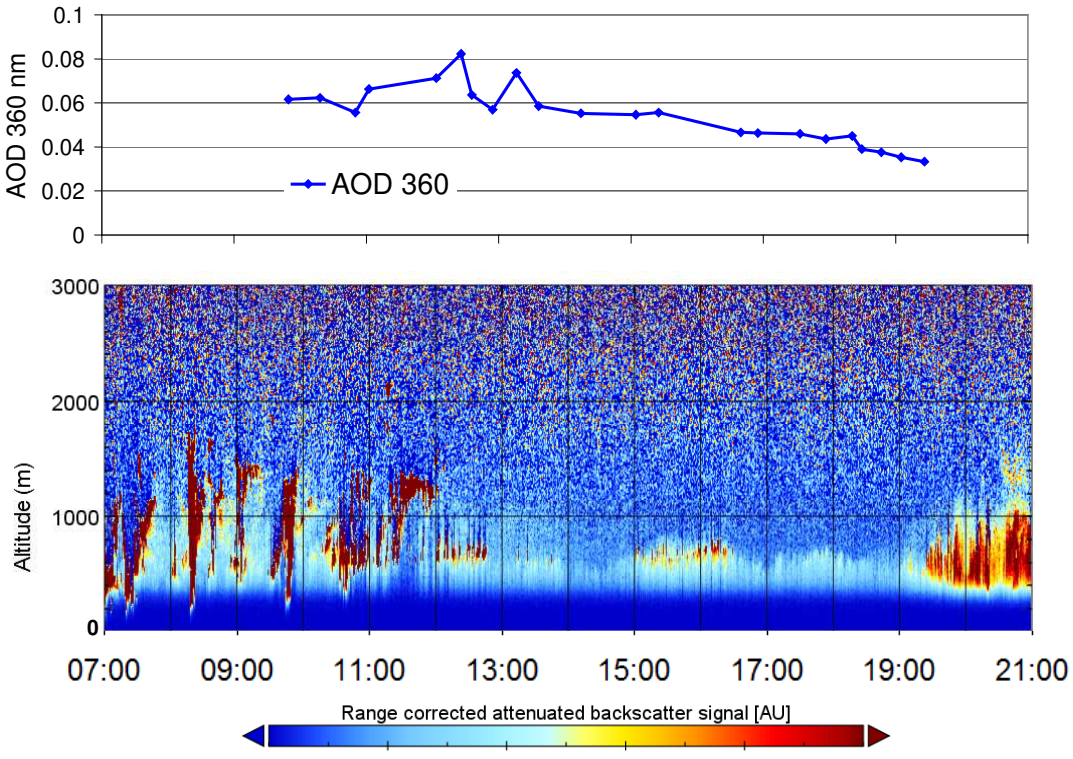

1210

Fig. 3: Top: AOD at 360 nm measured from the hand-held sun photometer. The data were extrapolated from the measurements at 380 nm using the Angström coefficient calculated from 380 nm and 440 nm. Bottom: Range-corrected ceilometer backscatter profile at 1064 nm.

1215

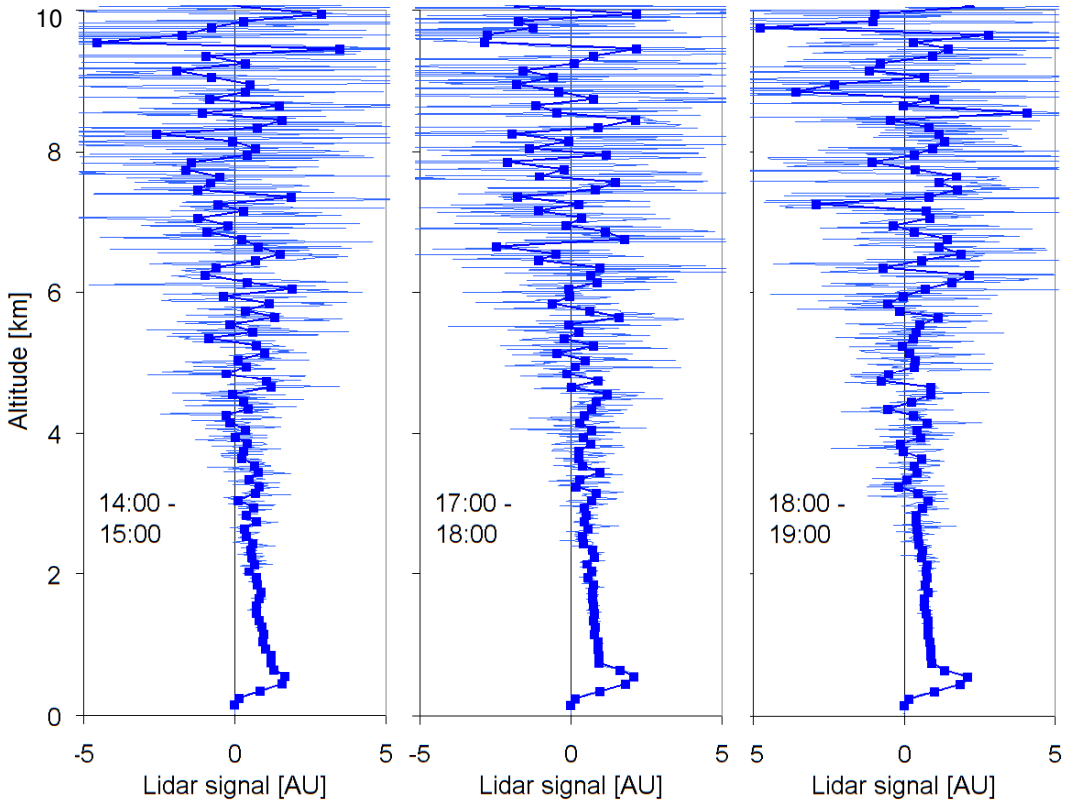

Fig. 4: Hourly averaged and range corrected ceilometer backscatter profiles for 3 periods on 2 May 2019 without cloud contamination. The thin lines represent the raw data. The dotted lines represent the smoothed profiles (averages over 100 m). The scatter of the range corrected backscatter profiles increases, because the received raw signal scales with the inverse of the square of the distance.

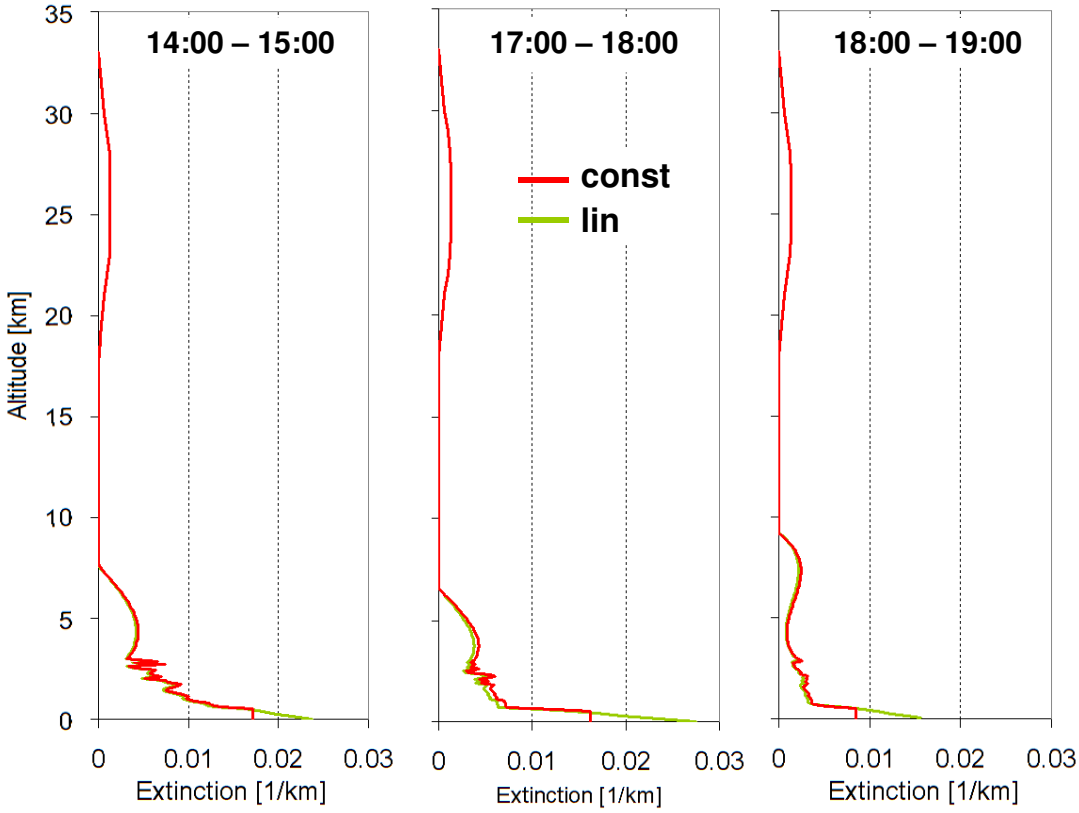

Fig. 5: Complete aerosol extinction profiles for the three time periods without clouds after all corrections are applied. The green curves represent the profiles with linear extrapolation below 500 m; the red curves represent profiles with constant values below 500 m.

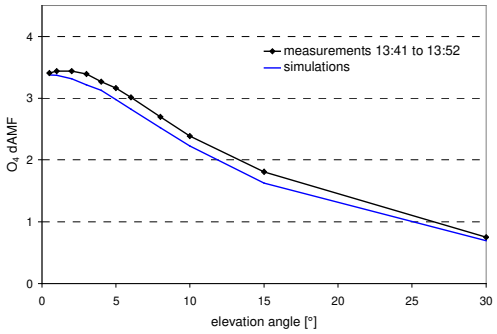
measurements 13:41 to 13:52
simulations
O4 dAMF
elevation angle [°]

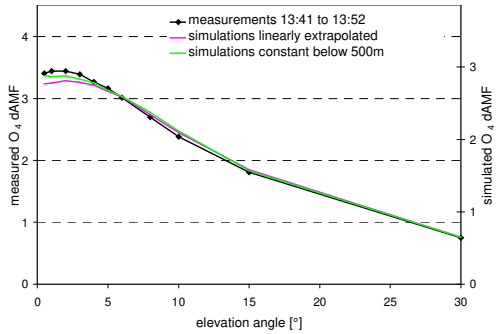
measurements 13:41 to 13:52
simulations linearly extrapolated
simulations constant below 500m
measured O4 dAMF
simulated O4 dAMF
elevation angle [°]

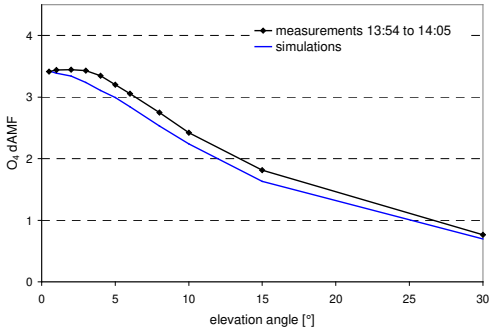
measurements 13:54 to 14:05
simulations
O4 dAMF
elevation angle [°]

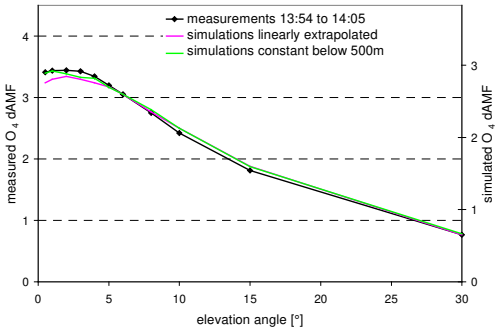
measurements 13:54 to 14:05
simulations linearly extrapolated
simulations constant below 500m
measured O4 dAMF
simulated O4 dAMF
elevation angle [°]

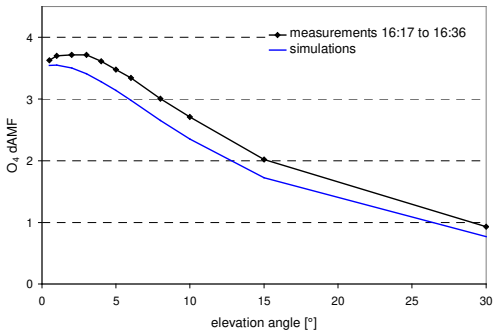
measurements 16:17 to 16:36
simulations
O4 dAMF
elevation angle [°]

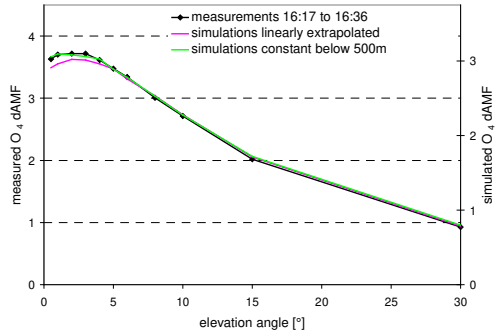
measurements 16:17 to 16:36
simulations linearly extrapolated
simulations constant below 500m
measured O4 dAMF
simulated O4 dAMF
elevation angle [°]

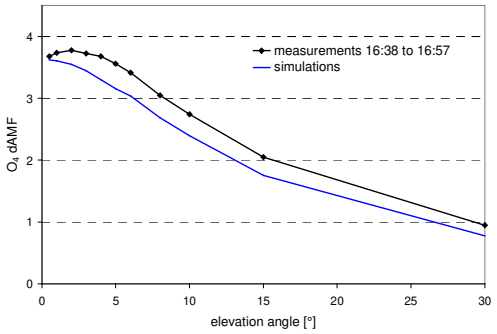
measurements 16:38 to 16:57
simulations
O4 dAMF
elevation angle [°]

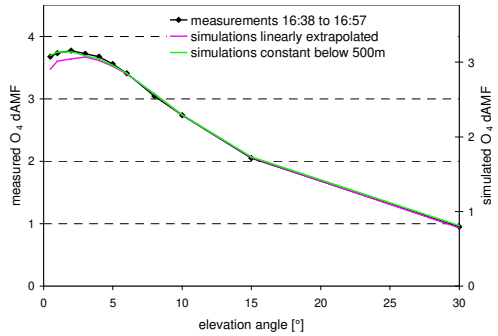
measurements 16:38 to 16:57
simulations linearly extrapolated
simulations constant below 500m
measured O4 dAMF
simulated O4 dAMF
elevation angle [°]

1275

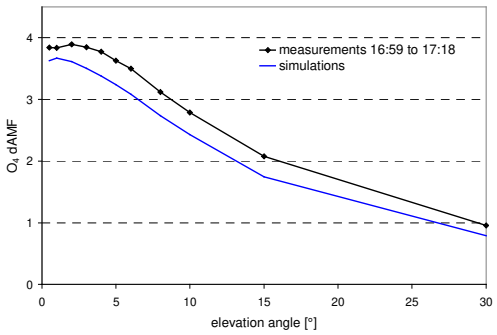
measurements 16:59 to 17:18
simulations
O4 dAMF
elevation angle [°]

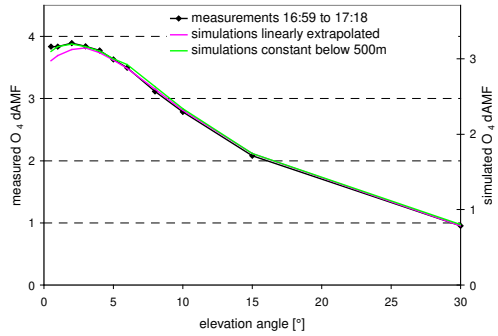
measurements 16:59 to 17:18
simulations linearly extrapolated
simulations constant below 500m
measured O4 dAMF
simulated O4 dAMF
elevation angle [°]

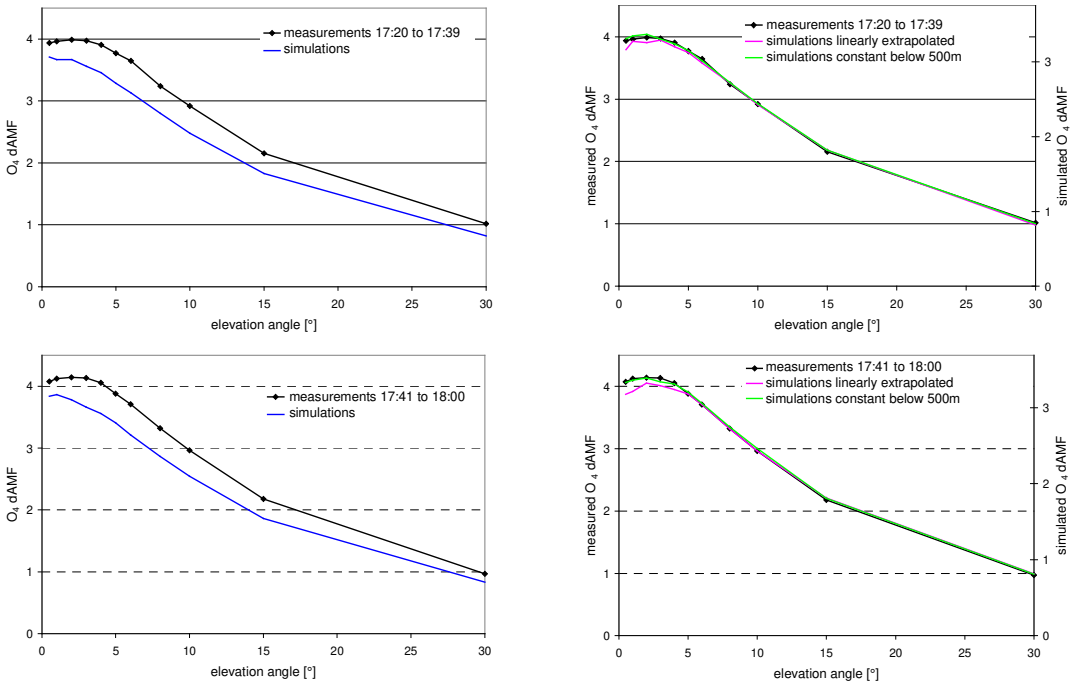

Fig. 6: Comparison of the measured and simulated O_4 dAMFs for selected elevation sequences without cloud contamination. In the left part, the measured O_4 dAMFs are compared to simulations for a pure Rayleigh atmosphere. In the right part they are compared to simulation results including aerosols (two profiles with either constant or linearly extrapolated aerosol extinction below 500 m). Note that in the right part separate y-axes on the right sides are used for the simulation results. The maxima of the right y-axes are chosen to achieve best agreement between the measured and simulated O_4 dAMFs (see text).

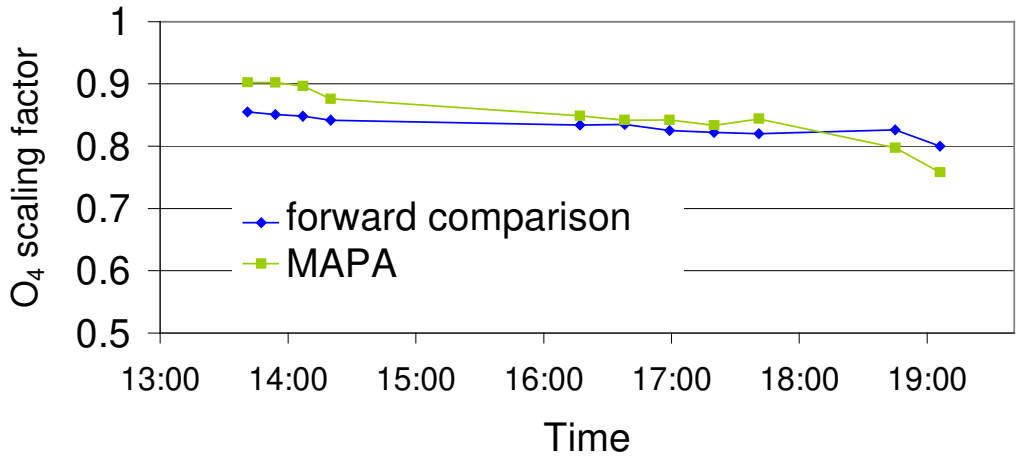

Fig. 7: Scaling factors derived from the direct comparison between the measured and simulated O_4 dSCDs (blue) and from the MAPA profile inversion (green) for all elevation sequences shown in Fig. 6 and Fig. ~~A11~~A12. Many of the measurements of the two last elevation sequences are affected by clouds. Note that for the last elevation sequence, the AOD used in the forward model has large uncertainties, see section 2.2.

Appendix A1 Effect of including a H_2O cross section or a second O_4 cross section on the retrieved O_4 dSCDs

H_2O cross section

Recent studies found evidence for substantial atmospheric H_2O absorptions in measured spectra in the UV (Lampel et al., 2017, Wang et al., 2017, 2020). These absorptions are usually rather small, but especially for measurement conditions with high atmospheric humidity the inclusion of a H_2O cross section in the spectral analysis can be useful.

Fig. A1 presents examples of the spectral analysis with either a H_2O cross section included or excluded. A clear H_2O absorption signal is found around 363 nm. The H_2O dSCDs retrieved at 363 nm agree reasonably well (r^2=0.63) with those retrieved at 442 nm (see Fig. A2) with a similar slope (2.07) as presented in Lampel et al. (2017) who found a slope of 2.39. If the H_2O cross section is not included in the analysis, a systematic structure appears in the residual. Thus, in this study, a water vapour cross section (Polyansky et al. 2018) is included in the spectral analysis. Here it should be noted that compared to other locations, the water vapour absorption during the ship cruise was rather high because most of the measurements were carried out under conditions of high atmospheric temperature and humidity. At other, colder locations, the impact of the H_2O absorption might be negligible.

Although the H_2O absorption is clearly found in the spectral analysis, the effect of including a H_2O cross section or not on the retrieved O_4 dSCDs is still rather small. If a H_2O cross section is included, the retrieved O_4 dSCDs are about 2.5 % larger than without a H_2O cross section included.

O_4 cross section at low temperature

We also investigated the effect of including a second O_4 cross section for low temperature (203 K). Before using this cross section in the fit it was orthogonalised with respect to the O_4 cross section at 293 K. Including the additional O_4 cross section leads to only small changes of the retrieved O_4 dSCD of about –1.5 %. Here it is interesting to note that the retrieved O_4 dSCDs for the O_4 cross section at low temperature were negative and the absolute values much smaller ($<2 \cdot 10^{43}$ molec^2/cm^5) than those at high temperature ($<6 \cdot 10^{43}$ molec^2/cm^5). The largest negative O_4 dSCDs for the O_4 cross section at low temperature were found indicating that the effective atmospheric temperatures decrease with elevation angle (see section 6.2). Also, the correlation between both O_4 dSCDs (r^2=0.20) is very low. Thus we conclude that the measured spectra do not contain significant O_4 absorptions at low temperatures. For the interpretation of this finding it should be noted that low temperatures exist only at higher atmospheric layers. The O_4 absorptions at these layers mostly cancel out in the spectral analysis, because the light paths of the measured spectra and the Fraunhofer reference spectra at these layers are very similar. This explains that the retrieved O_4 absorptions at cold temperatures are very small. To further confirm this hypothesis, we calculated the effective temperatures for the O_4 absorptions on 2 May 2019 (see section 6.2) and found them to be very close to the temperature of the high temperature O_4 cross section (293 K). Based on these findings, the O_4 results in this study are retrieved without including a second O_4 cross section at low temperature. It should, however, be noted that for measurements at other locations and seasons including a second O_4 cross section in the spectral analysis might be meaningful.

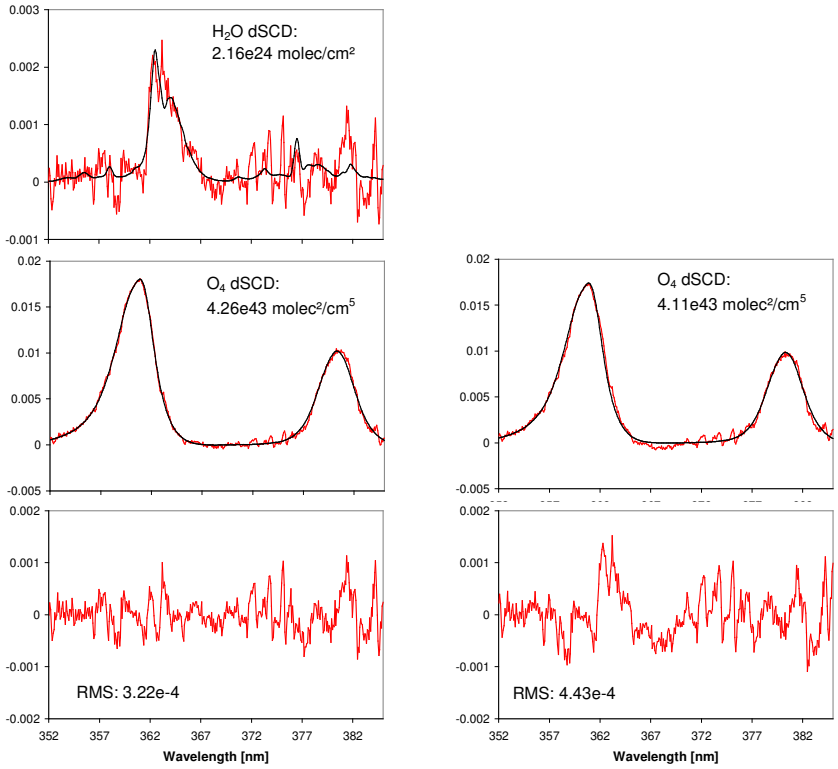

Fig. A1: Fit results for a spectrum taken on 2 May 2019, 13:14:50, at an elevation angle of 1° (SZA: 33.6°). Left: results if a H_2O cross section is included in the spectral analysis; right: results if no H_2O cross section is included in the spectral analysis. The black lines represent the fitted cross section, the red lines indicate the residual (bottom) or the residual plus the fitted cross section.

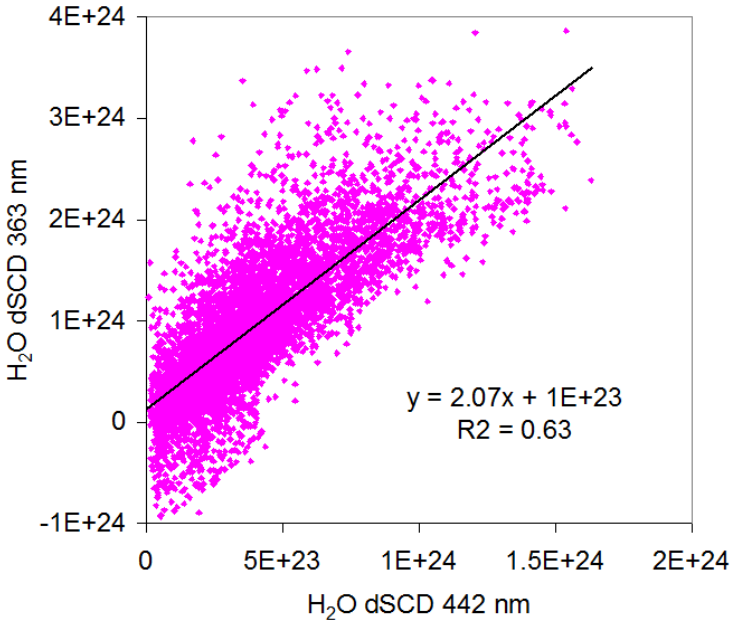

Fig. A2: Correlation plot of the H_2O dSCDs retrieved at 363 nm versus those retrieved at 442 nm for the whole ship cruise. The regression line is fitted assuming that the H_2O dSCDs retrieved at 442 nm have no error.

Appendix A2 Additional Figures

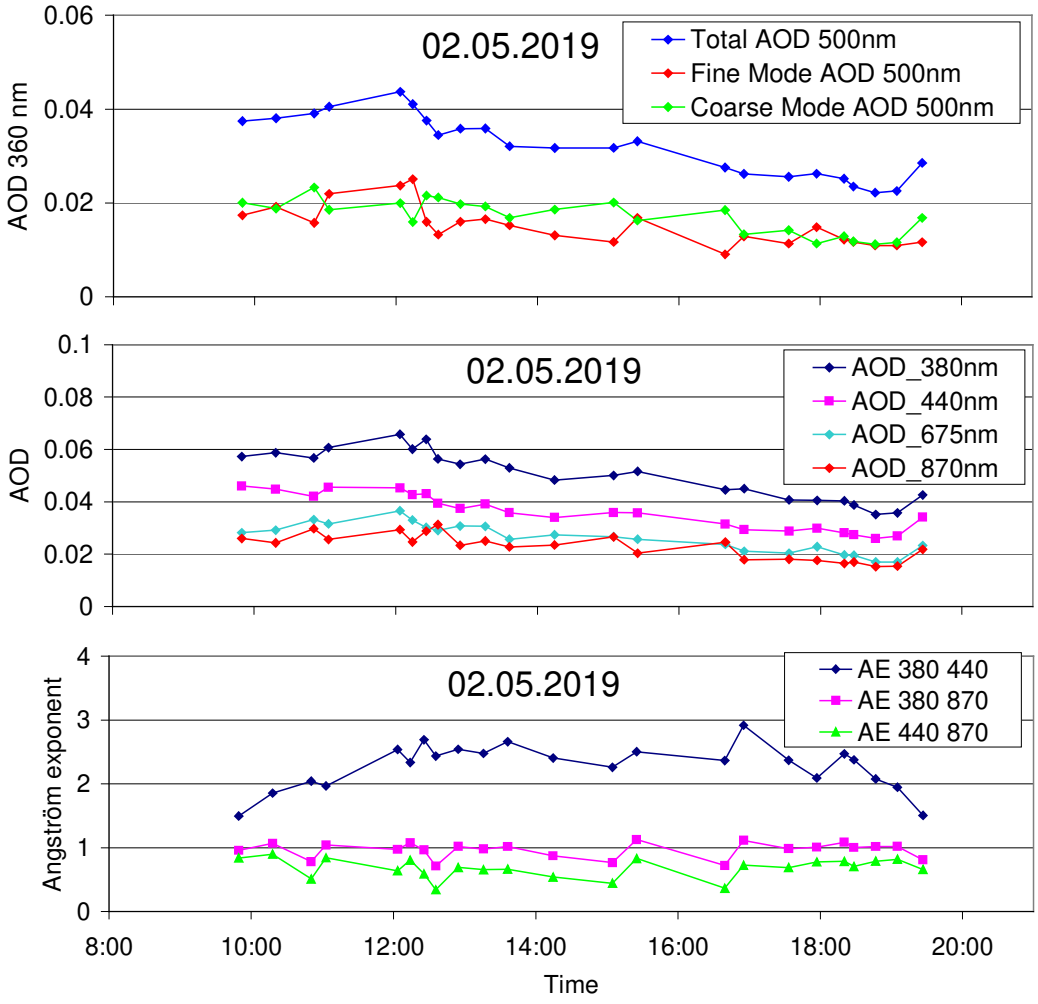

Fig. A3: Top: AOD at 500 nm attributed to the coarse and fine modes, as well as total AOD. Middle: Total AOD at different wavelengths. Bottom: Angström Exponents for selected wavelength pairs.

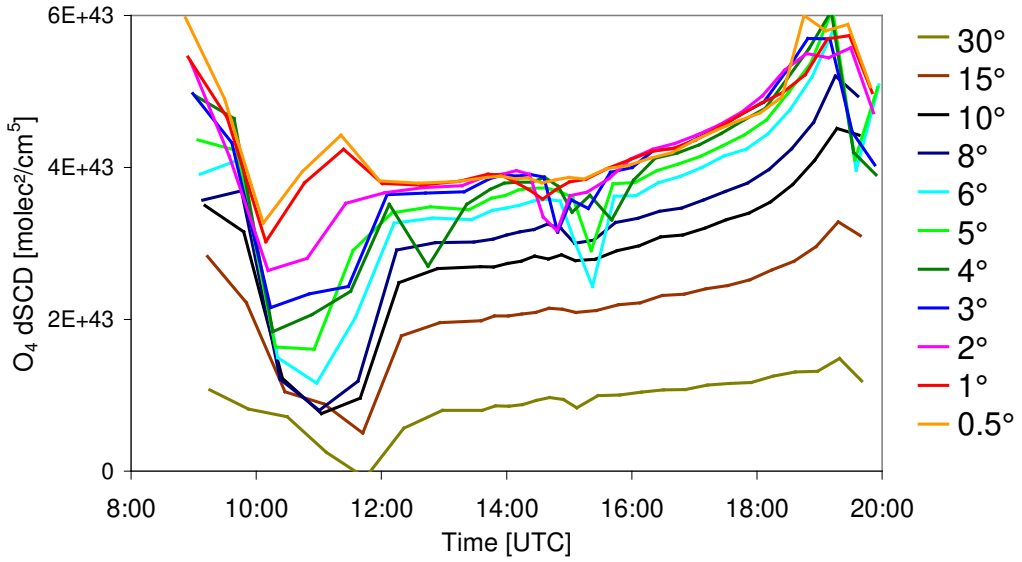

Fig. ~~A3~~A4: Time series of the retrieved O_4 dSCD on 2 May 2019 for the different elevation angles. During the afternoon, for most of the time smooth variations are found. However, for some times and elevation angles systematic deviations of the O_4 dSCDs occur, which are caused by scattered clouds.

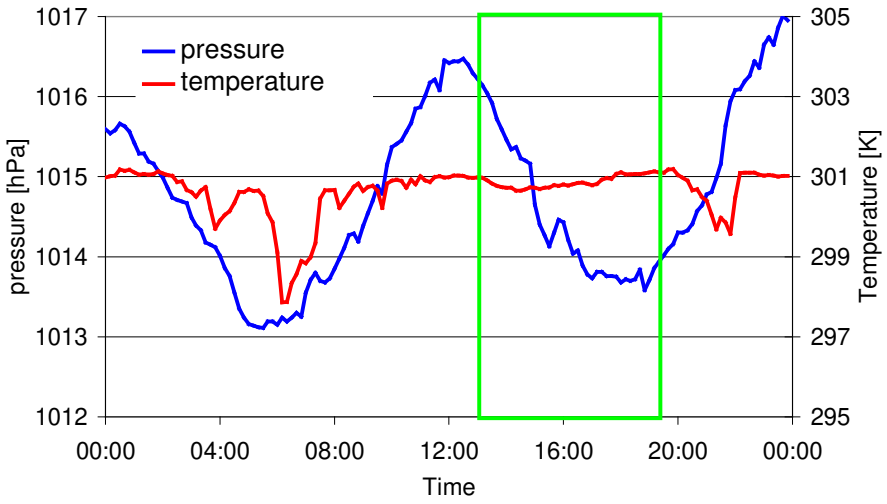

Fig. ~~A4~~A5: Diurnal variation of the surface pressure and temperature from in situ measurements on the ship. The green box indicates the period of the MAX-DOAS measurements used in this study. The corresponding values from the ECMWF model simulations are 1012.8 hPa and 299.8 K, respectively.

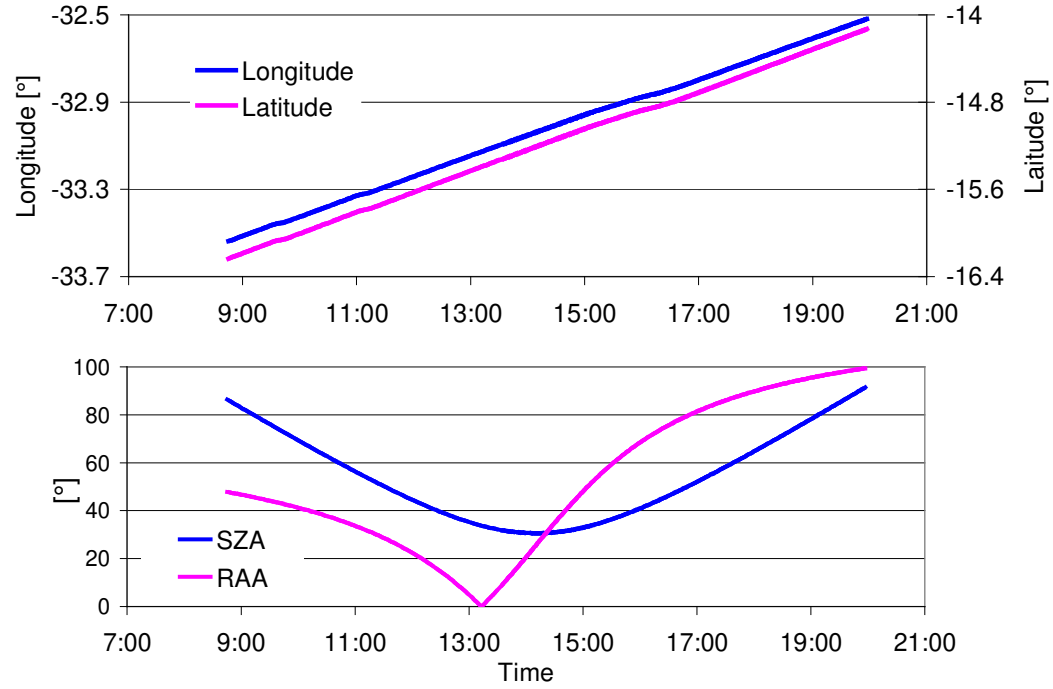

Fig. ~~A5~~A6: Top: Variation of the latitude and longitude of the ship position during 2 May 2019. Bottom: Corresponding variation of the SZA and relative azimuth angle (RAA).

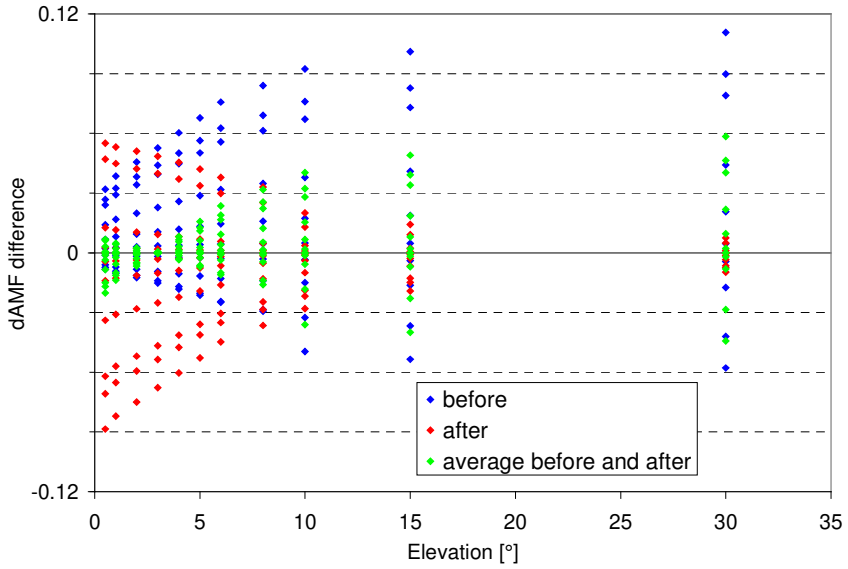

Fig. ~~A6~~A7: Effect of using different Fraunhofer reference spectra for the analysis of individual elevation sequences. Shown are the ratios of the obtained O_4 dSCDs for different selections versus those for Fraunhofer reference spectra interpolated between the zenith measurements before and after the selected elevation sequence. Before: zenith measurement before the sequence is used; After: zenith measurement before the sequence is used; Average before and after: the average of the zenith measurements before and after the sequence is used.

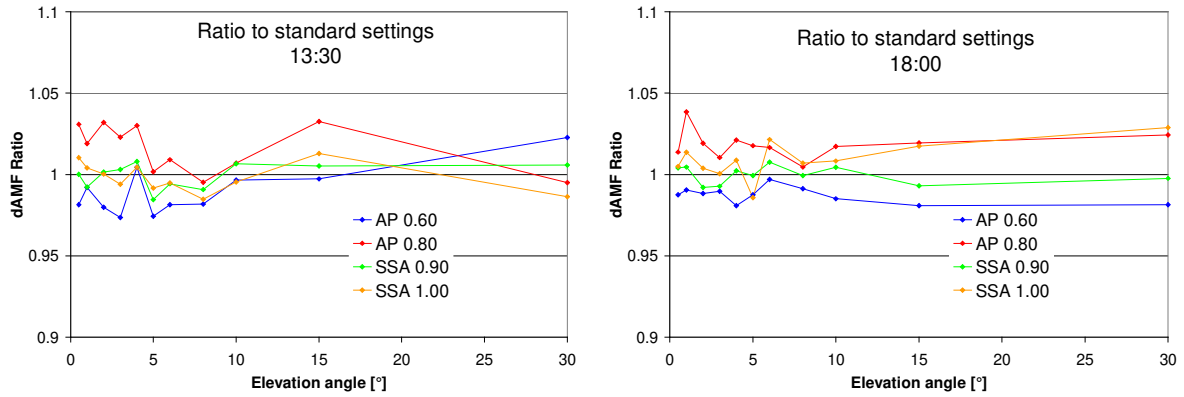

**Fig. ~~A7~~A8: Effect of different phase functions and single scattering albedos on the O_4 dSCDs. Shown are the ratios for simulations with variations of asymmetry parameter (AP) and single scattering albedo (SSA) versus simulations using the standard settings (AP= 0.68, SSA: 0.95). The results are for SZA of 33.6° and RAA of 0.7° (left, around 13:30) and SZA of 64.5° and RAA of 87.7° (right, around 18:00) on 2 May 2019~~). The results for other SZA/RAA combinations during the afternoon of 2 May 2019 are similar.

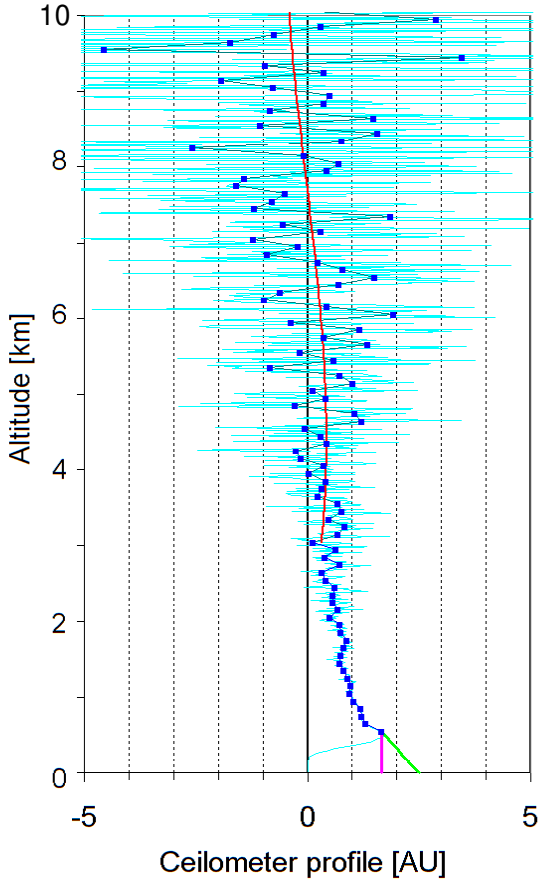

Fig. ~~A8~~A9: The light blue data show the original backscatter profile averaged between 14:00 and 15:00. The blue dots show the smoothed (with a 100m kernel) profile, which are used between 500 m and 3 km. Below 500m either constant or linearly extrapo~~l~~oated data (see te~~x~~t) are used. Between 3 km and 10 km a third order polynomial is fitted to the raw data. The polynomial values are used between 3 km and the altitude at which they become negative. Above, the values are set to zero.

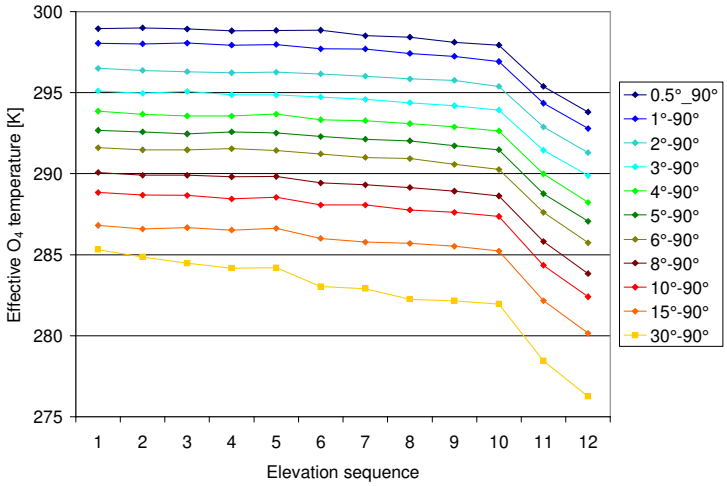

Fig. ~~A9~~A10: Effective temperatures calculated for the individual measurements according to equation 2.

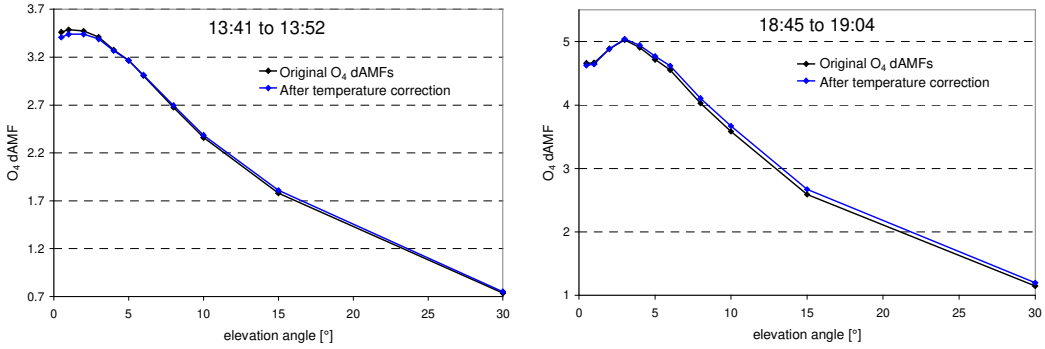

Fig. ~~A10~~A11: Effect of the temperature correction for two selected elevation sequences.

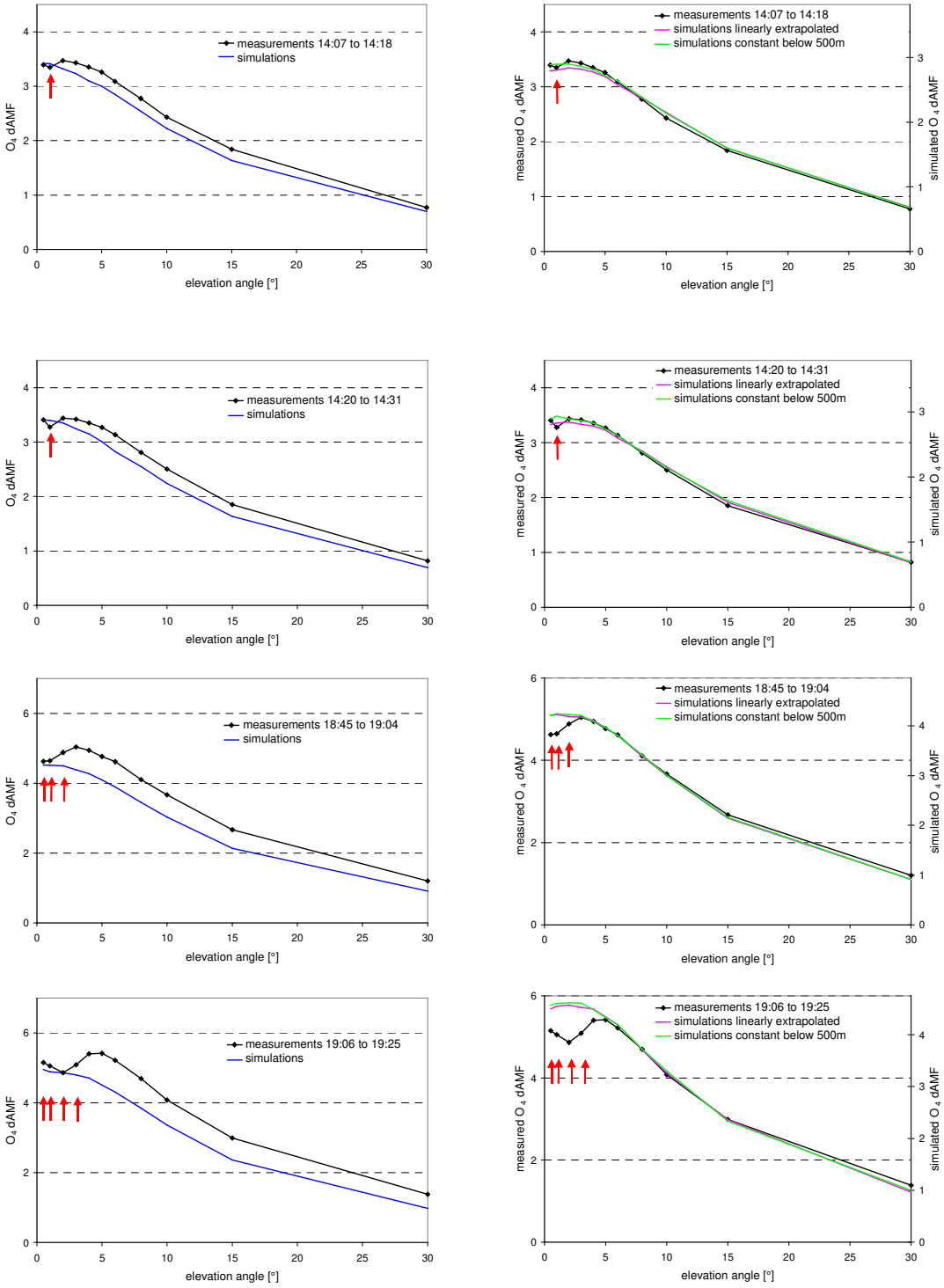

Fig ~~A11~~A12: Comparison of the measured and simulated O_4 dAMFs for five elevation sequences with few cloud-contaminated measurements (indicated by the red arrows). In the left part, the measured O_4 dAMFs are compared to simulations for a pure Rayleigh atmosphere. In the right part they are compared to simulation results including aerosols (two profiles with either constant or linearly extrap~~l~~olated aerosol extinction below 500 m). Note that in the right part separate y-axes on the right sides are used for the simulation results. The maxima of the right y-axes are chosen to achieve best agreement between the measured and simulated O_4 dAMFs (see text). Note that for the last elevation sequence (19:06 – 19:25), the AOD used in the forward model has large uncertainties, see section 2.2.

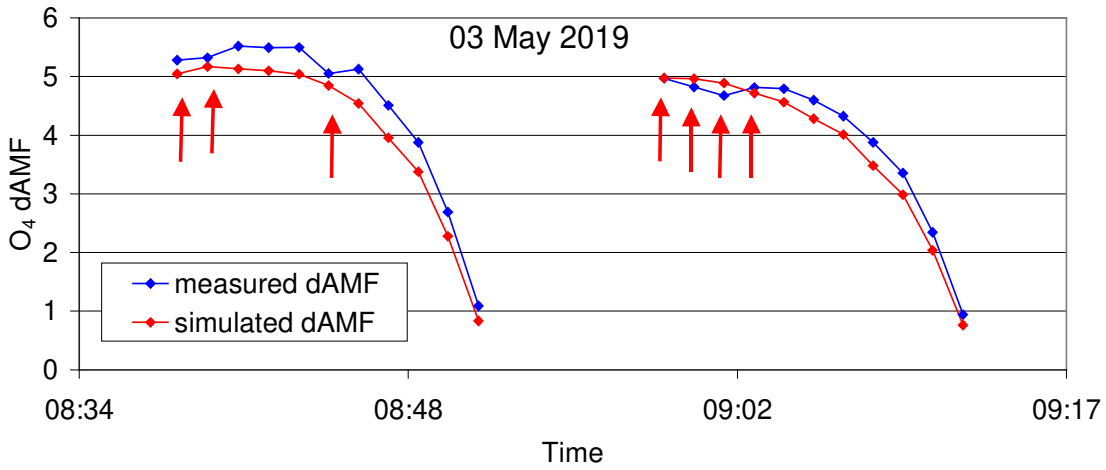

Fig A13: Comparison of the measured and simulated O_4 dAMFs for two elevation sequences on 05 March 2019. For the first elevation sequence, the AOD was <0.05 at 360 nm. During the second elevation sequence it already increased to 0.06. The radiative transfer simulations were made for an aerosol-free atmosphere. The red arrows indicate cloud-contaminated measurements.

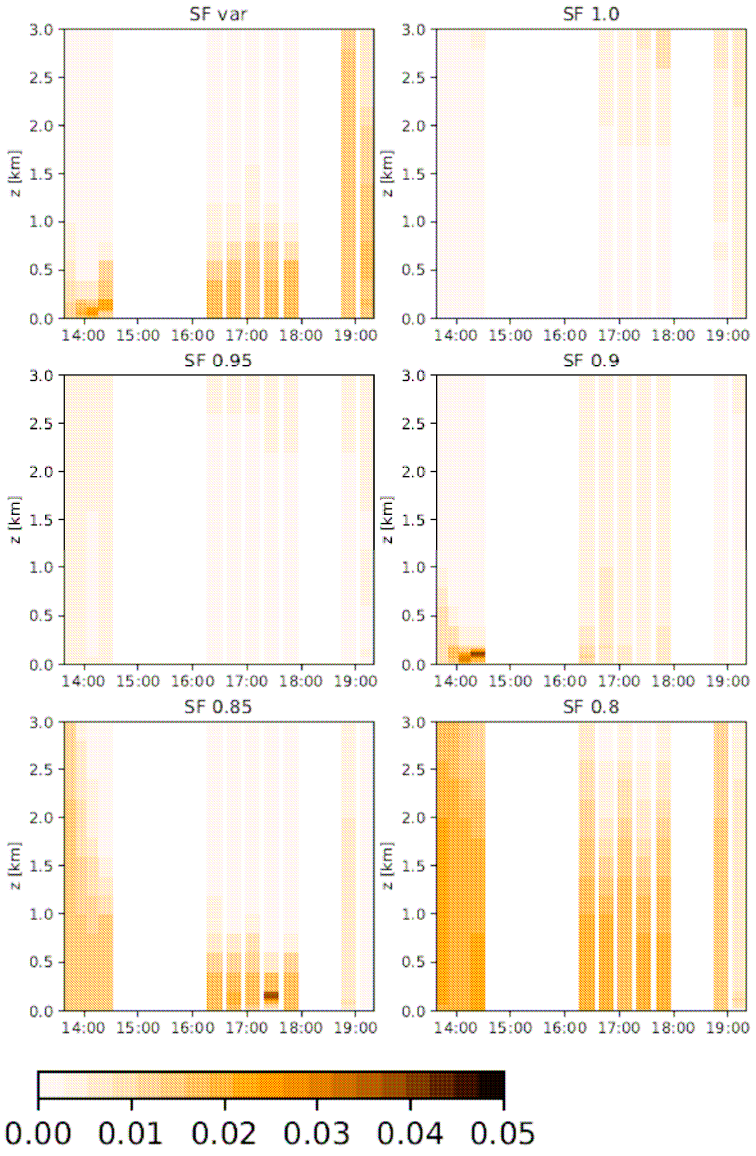

Fig A1~~2~~4: Extinction profiles retrieved with MAPA for the selected elevation sequences for different scaling factors. Only profiles for inversions with ‚valid' or ‚warning' flags are shown.

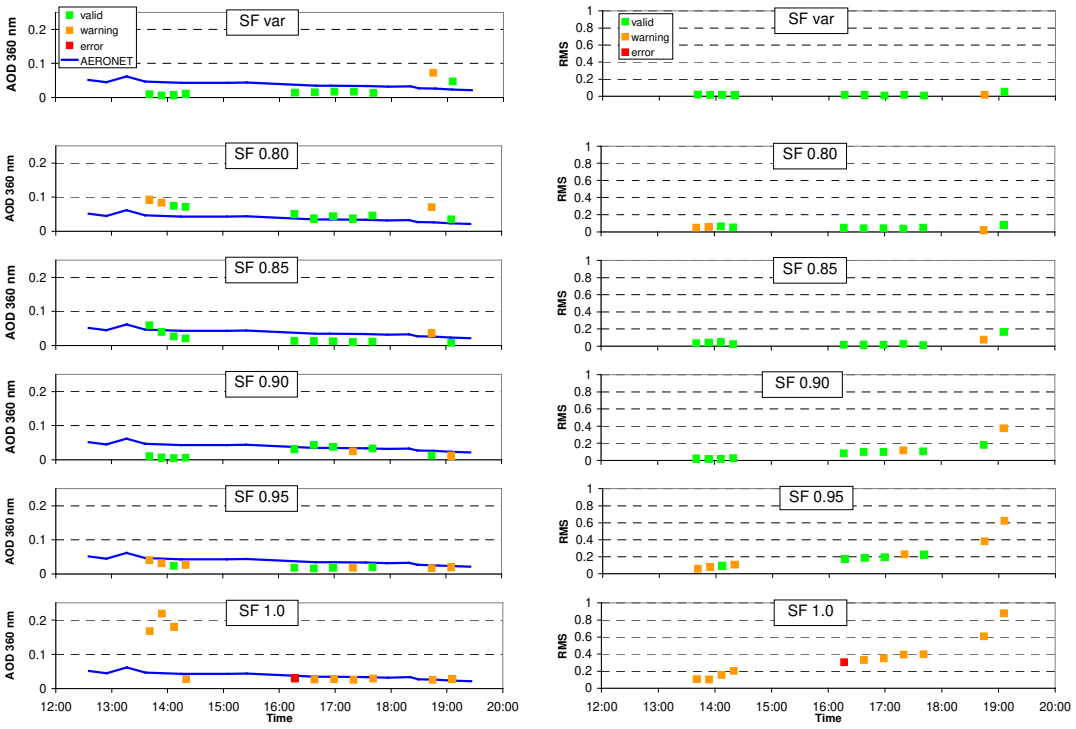

Fig ~~A13~~A15: Right: Comparison of the retrieved AOD for the MAPA profile inversions with different scaling factors (squares) and the (tropospheric) AOD observed by the sun photometer (blue lines). Right: RMS between the measured and fitted O_4 dAMFs. The colours indicate the quality flags for the individual profile inversions.

1495